CORE
Metadata, citation and similar papers at core.ac.uk
Provided by NASA Technical Reports Server

NASA CONTRACTOR REPORT

NASA CR-260

NASA CR-260

N65-27398
(ACCESSION NUMBER)
47
(PAGES)
(NASA CR OR TMX OR AD NUMBER)
1
(CODE)
07
(CATEGORY)
FACILITY FORM 602

GPO PRICE $ _____
CFSTI
OTS PRICE(S) $ 2.00

Hard copy (HC) _____
Microfiche (MF) .50

EXPERIMENTAL STUDIES OF THE TRAVELING-WAVE V-ANTENNA AND RELATED ANTENNAS

by Keigo Iizuka

Prepared under Grant No. NsG-579 *by*
HARVARD UNIVERSITY
Cambridge, Mass.
for

NATIONAL AERONAUTICS AND SPACE ADMINISTRATION • WASHINGTON, D. C. • JULY 1965

NASA CR-260

EXPERIMENTAL STUDIES OF THE TRAVELING-WAVE V-ANTENNA AND RELATED ANTENNAS

By Keigo Iizuka

Distribution of this report is provided in the interest of information exchange. Responsibility for the contents resides in the author or organization that prepared it.

Prepared under Grant No. NsG-579 by
HARVARD UNIVERSITY
Cambridge, Mass.

for

NATIONAL AERONAUTICS AND SPACE ADMINISTRATION

For sale by the Clearinghouse for Federal Scientific and Technical Information
Springfield, Virginia 22151 – Price $2.00

EXPERIMENTAL STUDIES OF THE TRAVELING-WAVE V-ANTENNA AND RELATED ANTENNAS

By Keigo Iizuka

Gordon McKay Laboratory, Harvard University
Cambridge, Massachusetts

SUMMARY

27398

This is a report on experimental investigation of the traveling-wave V-antenna. It includes a description of the apparatus, a discussion of the effect on the radiation patterns of variations in such quantities as the loading resistance R, the apex angle Δ, the length h of the traveling-wave section and the length h_T of the standing-wave section.

Tests were also made on traveling-wave V-antennas with more than one set of resistors and with more than two arms.

1. INTRODUCTION

A traveling-wave V-antenna consists of a V-antenna and a set of terminating resistors arranged near the ends of the antenna arms. With a proper value of resistance, the current on the antenna is substantially a wave traveling from the driving point to the terminating resistors. A traveling-wave V-antenna combines the advantages of a V-antenna and a traveling wave dipole. These include simplicity of structure, a broad frequency band, and high directivity with a pencil-type beam. There is, of course, a considerable loss of power in the terminating impedances. Since cylindrical symmetry does not obtain, the theoretical analysis is complicated.

The study includes a description of the apparatus, a discussion of the effect of (1) the unbalance in the excitation of the antenna, (2) changes in the location of the resistors from the end, (3) the length and the apex angle of the antenna, as well as a large number of the E- and H-plane patterns for different values of such quantities as loading resistance R, apex angle of the arms, Δ, the length h of traveling-wave section, and length h_T of the standing-wave section.

Traveling-wave V-antennas loaded with two sets of resistors and with a progressively increasing resistance were constructed and their characteristics were investigated experimentally. A four-armed traveling-wave V-antenna was also studied.

References are often made to the theoretical investigation on the traveling-wave V-antenna to be described in a later report.

2. EXPERIMENTAL SETUP

Figure 1 shows a general arrangement for measuring the field pattern of a traveling-wave V-antenna. The antennas were made of brass tubing 1/4 inch in diameter. The carbon film precision resistors (manufactured by Aerovox Corporation in USA), 1/4 inch in diameter, were held between two finger pieces, the one attached to the top section, the other to the bottom section of the antenna (see Fig. 1). It was possible to change the length of the antenna by inserting or removing otherwise identical sections of brass tubing of different lengths. The tips of the top sections of these tubes were plugged with hemispherical caps. The driving-point ends (receiving point) were connected to a short two-wire line section by means of a set of hinges so that the apex angle Δ of the V-antenna could be varied. The two-wire feeder line was provided with a tuning stub for the balanced component of current, a suppressor for the unbalanced component, an unbalance indicator, and output terminals to the balun. Both the antenna and the two-wire transmission line were secured on blocks of expanded polystyrene which were supported on a wooden frame on a turntable. The top block of the expanded polystyrene had a number of long radial 1/4 inch wide grooves on the flat surface on which both arms of the V-antenna were secured with the desired apex angle Δ. The top block could be mounted either vertically or horizontally on the turntable for pattern measurements in the E plane or H plane. The entire block of expanded polystyrene could be raised from about 2.5λ to 3.9λ wavelengths by inserting extra blocks of expanded polystyrene between the original blocks and the wooden frame in order to determine the effect of the "ground." The experiments were performed on the roof of the five-story high laboratory building which is one of the highest structures in the vicinity. (Among the buildings in the direction of the propagation of the incident wave it is the highest.) The turntable was placed on the top of the penthouse, the highest point of the roof, and the transmitting antenna with a parabolic reflector was placed directly on the surface of the flat roof, so that a wave reaching the test-receiving antenna by a single reflection from the surface of the roof was minimized. The transmitting antenna was excited at 600 Mc/s (50 cm in wavelength). The signal received by the traveling-wave V-antenna was fed into a balun through the two-wire transmission line. The balun served to convert from a two-wire transmission line to a coaxial line. A small dipole probe perpendicular to the two-wire line in its neutral plane was used to check the balance of the excitation on the two-wire line. The probe was mounted on a polystyrene carriage which could be slid along the two-wire line in the neutral plane.

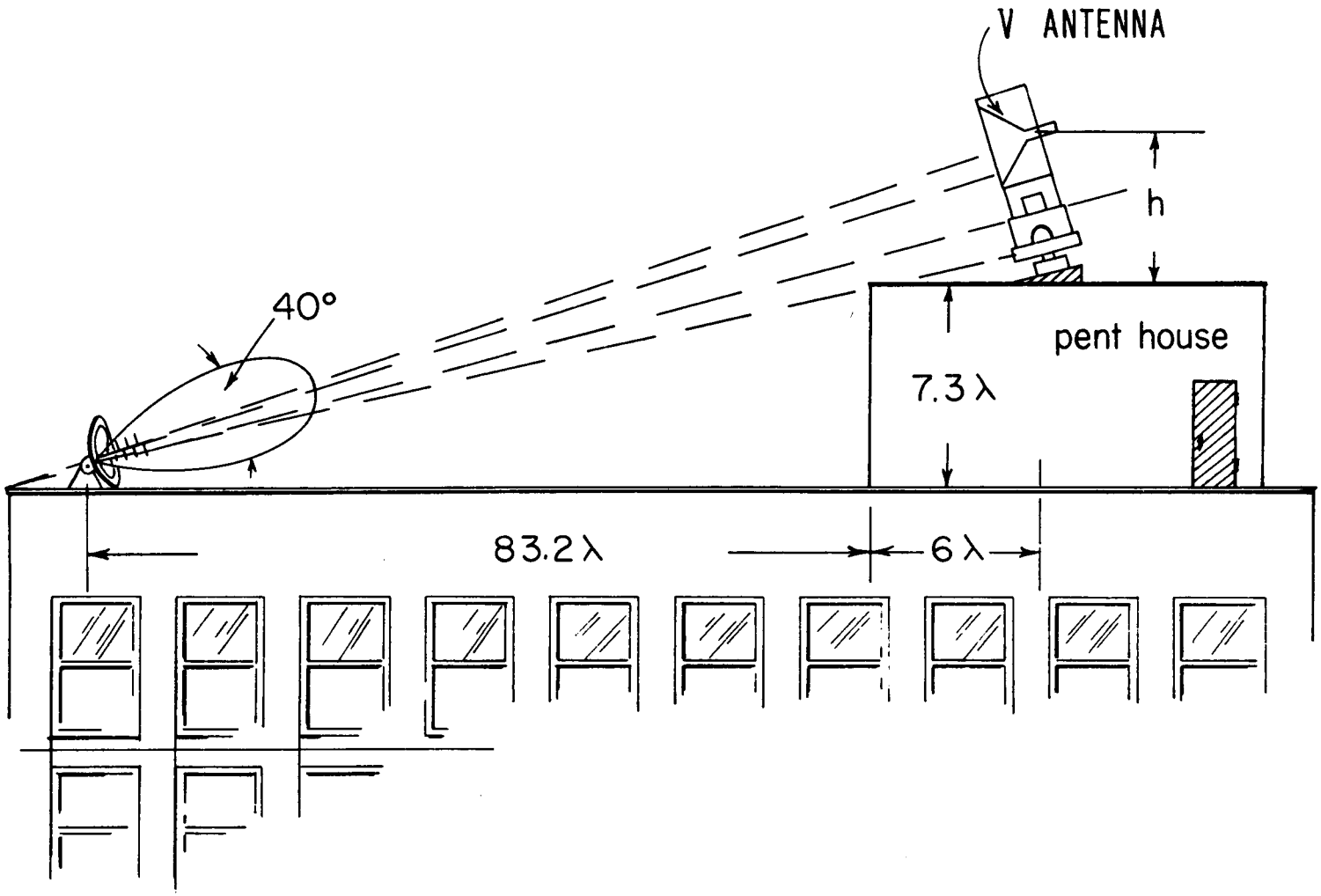

FIG. 1 SCHEMATIC OF THE EXPERIMENTAL ARRANGEMENT FOR MEASURING THE FIELD PATTERN OF A TRAVELING-WAVE V-ANTENNA.

3. BALANCED EXCITATION

The effects of an unbalanced component of current on the distribution of the current along the antenna fed to (or driven by a two-wire transmission line, have often been overlooked. It is of significance when the experimental results are to be compared with theory which assumes that the two-wire line (and antenna) are driven in a manner to excite only balanced or transmission-line mode currents with equal magnitudes and 180° phase differences at corresponding points in the two wires and in the arms of the V-antenna. Unbalanced currents with equal magnitudes and phases at the corresponding points are assumed absent. Owing to the radiating properties of the unbalanced current, the two-wire transmission line and other feeding lines connected with it become a part of the radiating system when they are excited predominantly by unbalanced currents and it becomes difficult to perform the experiments. Moreover, any imperfection in the balance of the balun contributes to the unbalanced component of current and gives an error in the output of the balun. Consider the configuration shown in Fig. 2a. The plane of the antenna coincides with the E plane of the incident wave. It is evident that the current I_{t_1} on arm 1 and I_{t_2} on arm 2 are not equal. The difference between these currents constitutes the unbalanced component I_u. More quantitatively speaking, the current I_{t_1} and I_{t_2} can be decomposed into the balanced and unbalanced components of current I_b and I_u.

$$I_{t_1} = I_b + I_u \tag{1}$$

$$I_{t_2} = I_b - I_u \tag{2}$$

or

$$I_b = \frac{1}{2} (I_{t_1} + I_{t_2}) \tag{3}$$

$$I_u = \frac{1}{2} (I_{t_1} - I_{t_2}) \tag{4}$$

The configuration of the excitation by the balanced and unbalanced components of current is shown in Fig. 2b and 2c. When a receiving system is connected between A and A' the optimum power transmission into the receiving system can be obtained by placing short-circuits at the proper points. As for the suppression of the unbalanced currents, the magnitude of I_u is a periodic function of the total length ℓ (antenna and feeder) with maximum (resonance) and minimum (antiresonance) appearing successively and alternately as the total length ℓ is increased. The value of ℓ was adjusted to the length of the minimum excitation of I_u by expanding or contracting a trombone section D in Fig. 2 at the end of the two-wire transmission line. (Note that the short-circuits BB' and CC' contribute nothing to the balanced current components, since they join equipotential points.)

The magnitude of I_u was monitored by a short dipole probe in the neutral plane of the transmission line. The dipole probe was placed perpendicular to the transmission line and, hence, in the neutral plane for the balanced currents but highly sensitive to the charges in the unbalanced mode. Since the probe is also perpendicular to the incident field it does not respond to this.

This configuration gives better sensitivity to the charges on the transmission line because the component of the E field normal to the transmission line is much greater than that tangential to it at points very close to the transmission line. A sketch of the balancing section is shown in Fig. 3. The dipole probe was placed at about 1/2 wavelength away from the end of the transmission line where the maximum of the unbalanced current was normally located.

Figure 4 shows measurements made to determine the excitation of the unbalanced current (power in an arbitrary linear scale) as a function of the total length ℓ. The dimension of the arm of the traveling-wave V-antenna used was $h = \lambda$ and that of the top section $h_T = \lambda/4$; the apex angle was $\Delta = 10^o$ and the loading resistance was $R = 250$ ohms. The total length, ℓ, was changed from $\ell = 113$ to 125 cm by successively expanding the trombone section at intervals of a twenty-fifth of a wavelength. The antenna was oriented at $\phi = 152^o$ with respect to the incident wave. (This angle was empirically found to be the angle of the largest excitation of the unbalanced current component between $\phi = 0$ and 180^o for the antenna with above dimensions. There were four other angles between $\phi = 0$ and 180^o at which the excitation of the unbalanced current reached a maximum but the peak at $\phi = 152^o$ was the largest and the position of the peak was insensitive to changes in the value of ℓ.) It is seen from the figure that the power in the unbalanced current changes rather significantly with respect to the total length, and in the range covered the excitation of the unbalanced current could be cut down by roughly half of the worst case by selecting the optimum length.

It is interesting to note that the minimum excitation of the unbalanced current occurs at lengths only slightly longer than $9\lambda/4$ which is the anti-resonant length of a thin straight wire. (When a piece of straight wire was exposed to an incident wave the magnitude of the excited current on the wire changed with its length. The word anti-resonant was used in the sense of that length for which the magnitude of the excited current on the wire was smallest.)

After selecting the optimum length of the trombone section D by monitoring the output of the unbalanced probe, the short-circuit section AA' was adjusted to the optimum output from the detecting system.

Figure 5 shows radiation patterns for various ratios of unbalanced to balanced currents. The radiation patterns in the E plane (in the plane

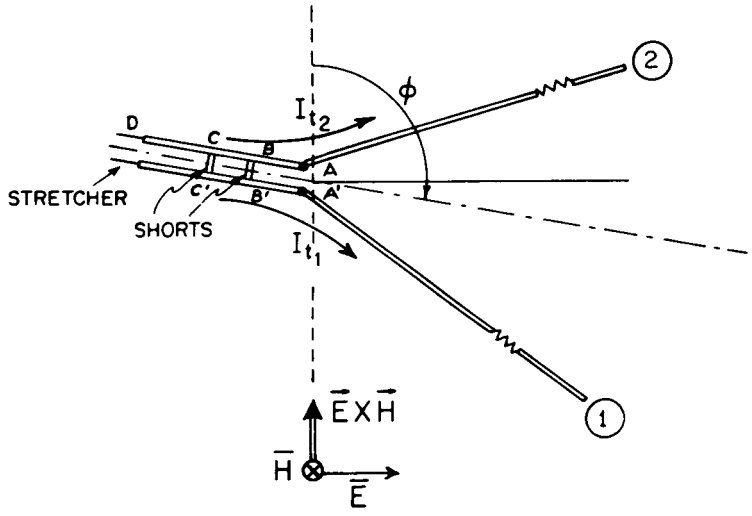

FIG. 2a EXCITATION OF CURRENT.

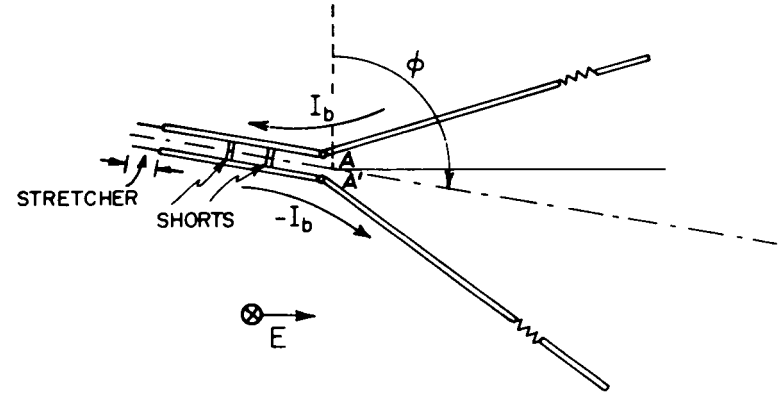

FIG. 2b BALANCED COMPONENT OF CURRENT.

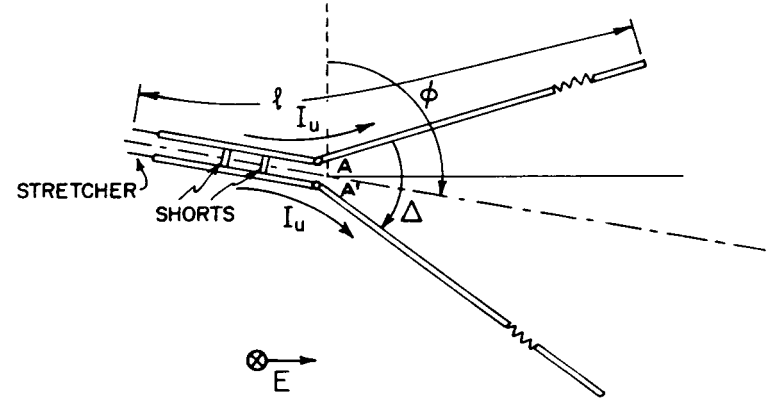

FIG. 2c UNBALANCED COMPONENT OF CURRENT.

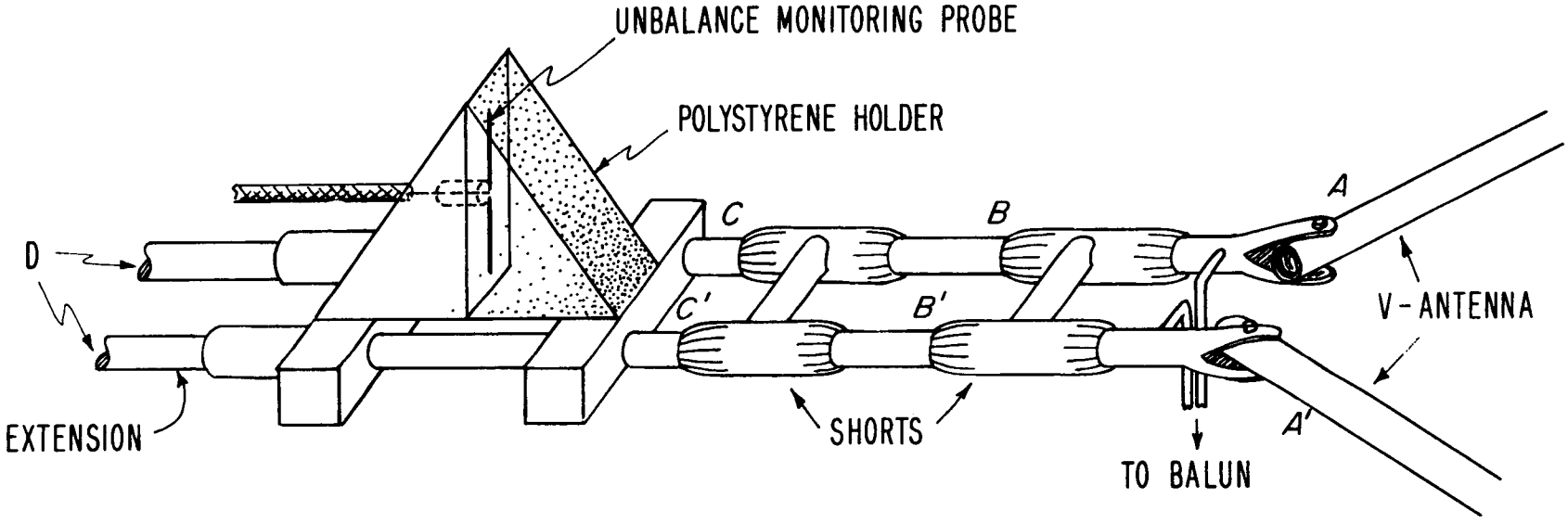

FIG. 3 SKETCH OF THE BALANCING MECHANISM.

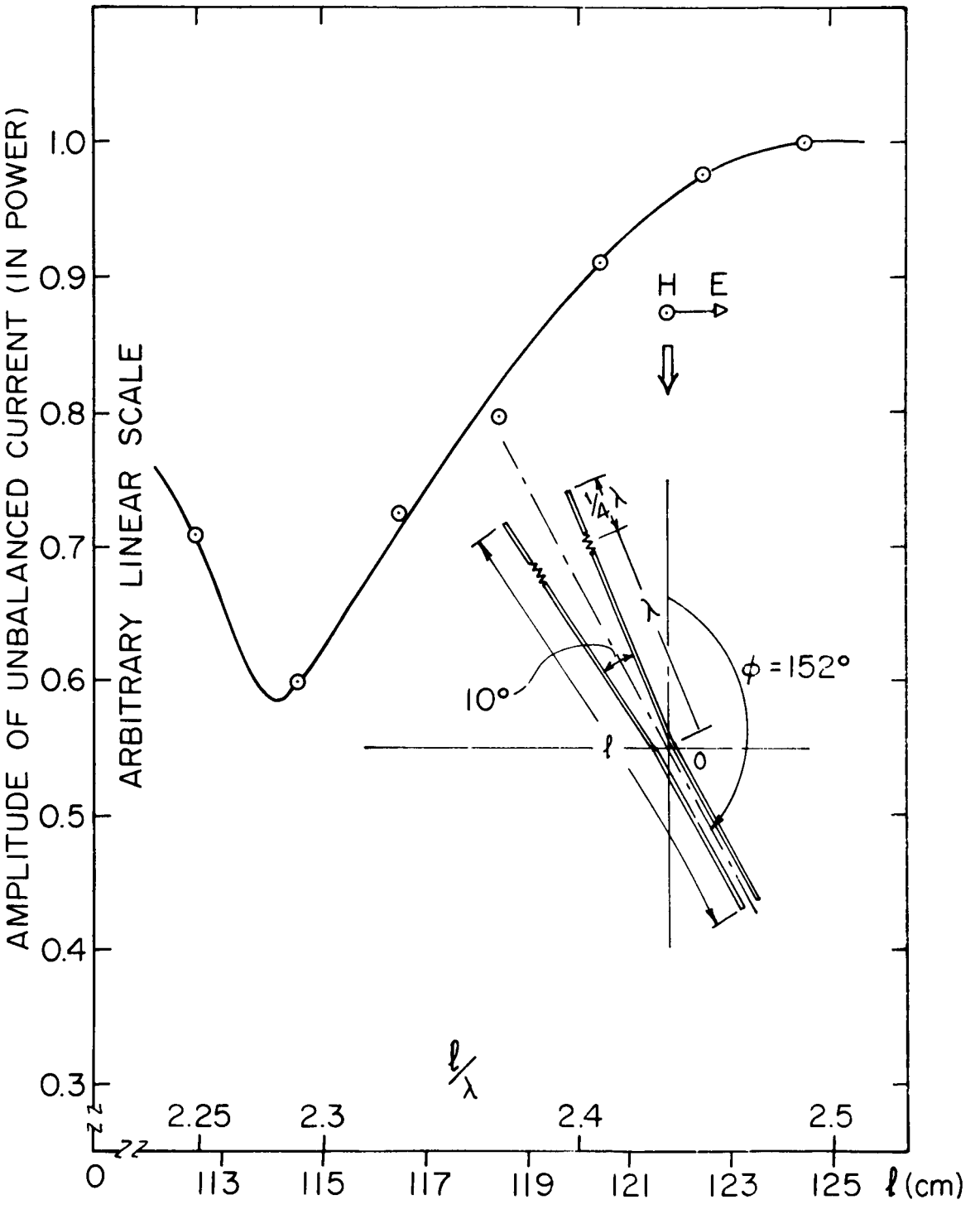

FIG. 4 AMPLITUDE OF THE UNBALANCED CURRENT AS A FUNCTION OF THE TOTAL LENGTH ℓ OF THE ANTENNA AND THE TRANSMISSION LINE.

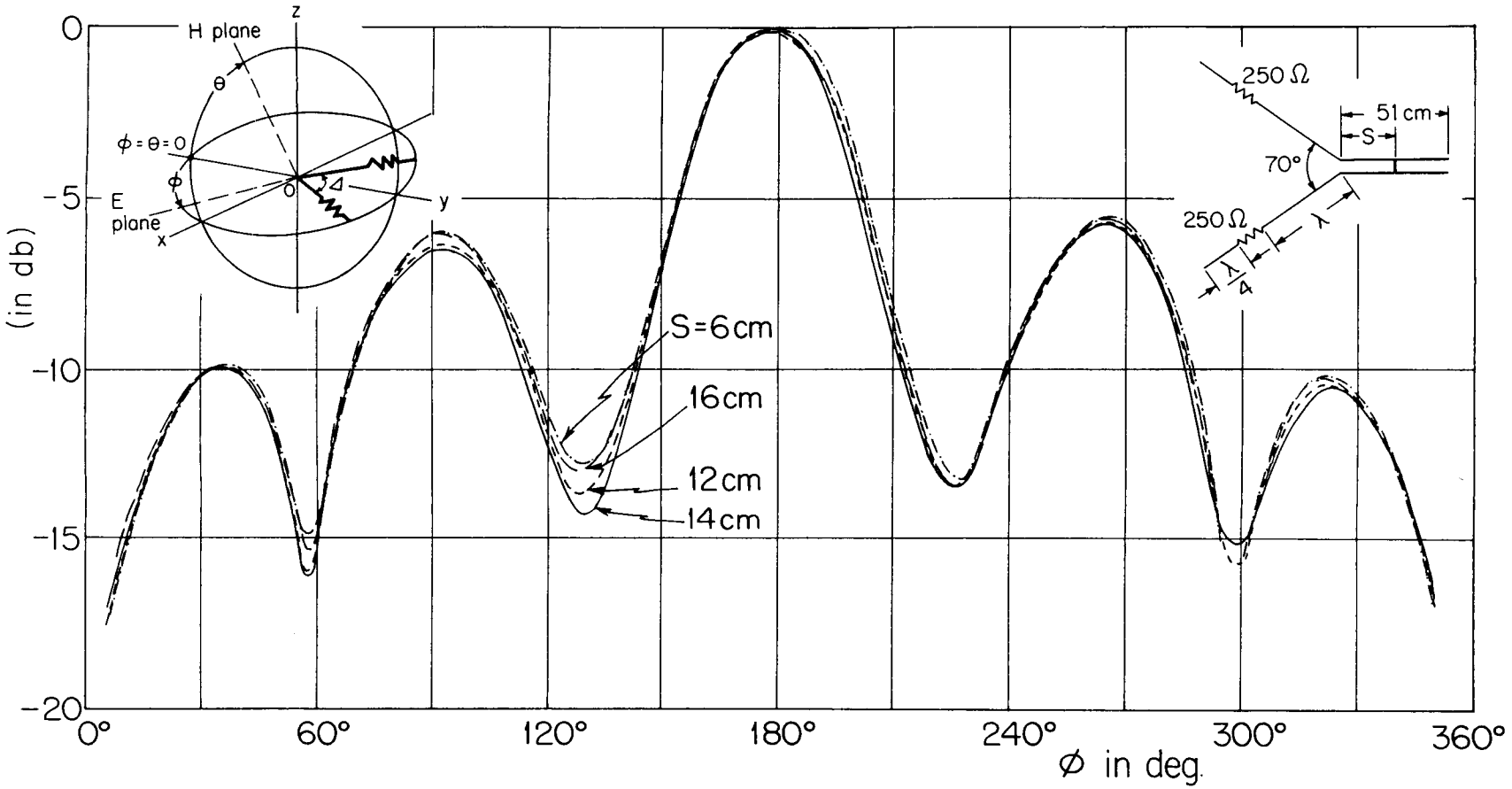

FIG. 5 RADIATION PATTERN WITH VARIOUS RATIOS OF I_u/I_b ON A TRAVELING-WAVE V-ANTENNA. (E PLANE)

of the antenna or ϕ variation in the coordinate system shown in Fig. 5) of a traveling-wave V-antenna with $h = \lambda$, $h_T = \lambda/4$, $\Delta = 70^o$ and $R = 250$ ohms were repeatedly measured with different settings of the tuning device B-B' for the balanced current I_b. This is to measure the patterns of the antenna with different ratios of the unbalanced current I_u/I_b. Only very little difference in the shapes of the radiation patterns could be observed. The maximum differences were located near the direction of the minimum radiation but they are within 0.5 dB. The symmetry of the pattern with respect to $\phi = 180^o$ is also preserved. This can be interpreted to mean that the contribution of the unbalanced current to the radiation pattern is reduced sufficiently to be negligible, because the radiation patterns show very little change when the ratio I_u/I_b of the unbalanced component to that of the balanced component is increased. This is a consequence of the fact that the absolute value of I_u had already been reduced to make it very small.

4. EFFECT OF THE GROUND

The study of the effect of the reflection from the roof on the measured radiation pattern is essential for determining the fidelity of the measured shapes of very low side lobes. A simple criterion based on the asymmetry of the measured pattern is not enough since most of the reflections from the ground are symmetric with respect to the line which connects the transmitter and the turntable when the experiments are performed in the open area.

The field at the point in the aperture of the test antenna is the vector sum of the direct-path field and the wave due to reflections from the surface of the roof. The relative phases of the direct and reflected signals vary with positions over the aperture of the test antenna. In the configuration for which the beam maxima of the transmitting and test antennas are directed toward each other, the effect of the reflected signal is the least owing to the directivity of the antennas in addition to the attenuation due to the reflection from the roof surface. When, however, the peak of the pattern of the test antenna was directed toward the directly reflected wave, the reception of the direct-path signal was reduced and that of the reflected signal increased so that the measured level could deviate up to ∞ dB from the true level. Due to the above effects, the measurement of the E-plane radiation pattern in the present arrangement is subject to greater error than is the radiation pattern in the H plane. The error involved in the E-plane measurements has been investigated quantitatively in order to determine the maximum error. In Fig. 6 are shown the radiation patterns of the same antenna ($h = \lambda$, $h_T = \lambda/4$, $\Delta = 70^\circ$, and $R = 250$ ohms) when at different heights H above the ground. It is seen from the figure that the shapes of the minor lobes are significantly changed with a decrease in height (even though they fairly well preserve the symmetry of the pattern with respect to ϕ to the lowest height of the antenna).

The largest asymmetries are found near the direction of minimum reception and increase to an average of 2 to 2.5 dB for the two lowest heights H of the antenna $H = 2.52\lambda$ and 3.49λ and 0.7 dB (8% in magnitude) for the highest antenna $H = 3.93\lambda$. The pattern for the second highest antenna is like that of the highest antenna except for a 2.5 dB deviation near $\phi = 230^\circ$ and with an average of 0.5 to 0.7 dB (6 to 8 % in magnitude) deviation. The patterns of the longer antennas had to be measured at the second highest location $H = 3.49\lambda$ to maintain the requisite mechanical stability of the support against the wind. These measurements are subject to error by the power level discussed above.

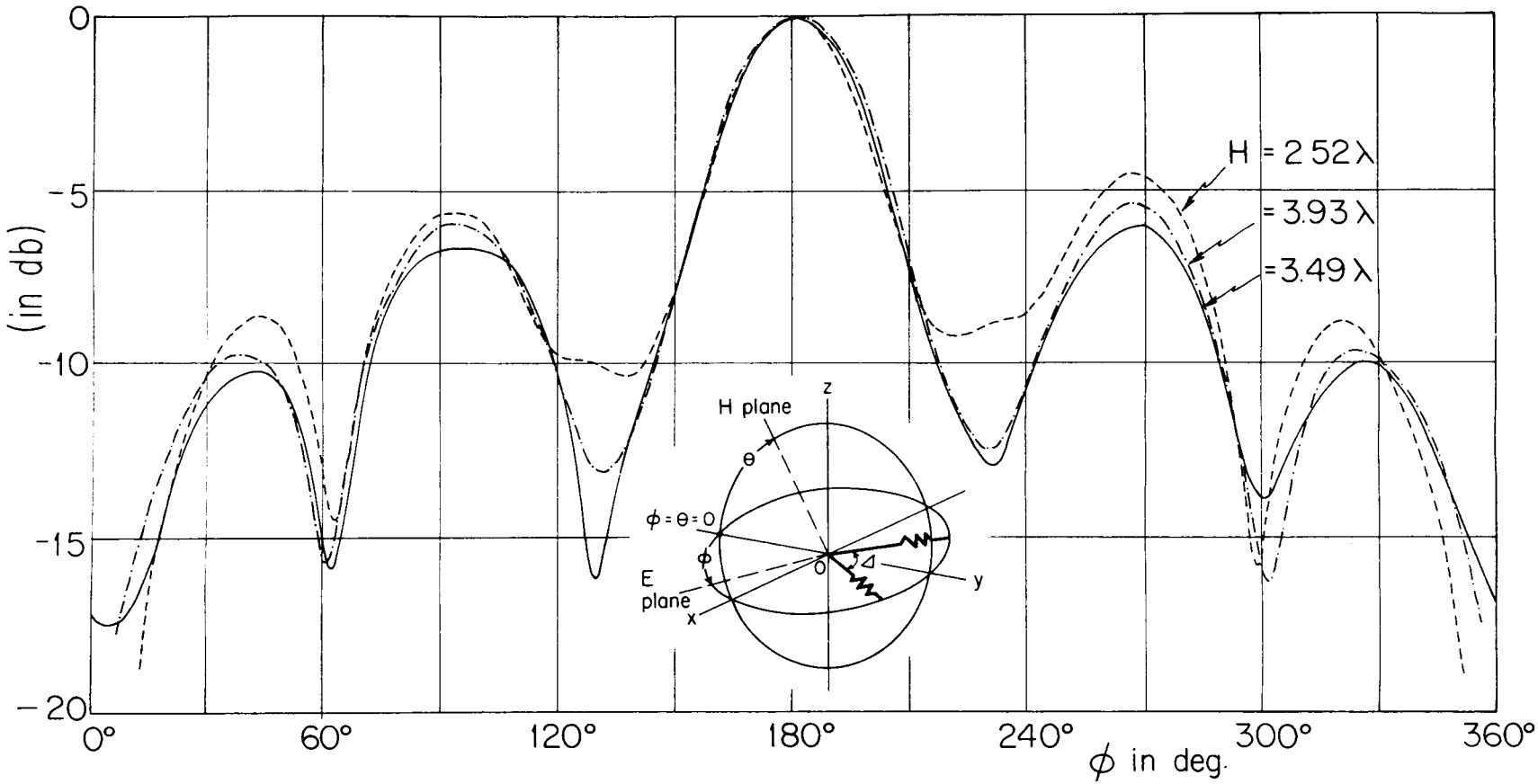

FIG. 6 RADIATION PATTERN OF THE SAME ANTENNA WITH DIFFERENT HEIGHTS, H OF THE ANTENNA ABOVE THE GROUND TO CHECK THE EFFECT OF THE REFLECTION FROM THE GROUND. (E PLANE)

5. EXPERIMENTAL RESULTS

The theoretical computation of the radiation pattern, directivity, and power gain in a separate report has assumed a sinusoidal traveling-wave excitation along the antenna. Therefore, although the radiation pattern of a V-antenna when excited by a predominantly sinusoidal traveling wave, may be predicted with reasonable accuracy, no theory is available when the excitation departs greatly from a traveling-wave current. The purpose of the experiments, therefore, is threefold: (1) to verify the theoretically obtained results by exciting the antenna essentially by a traveling-current wave, (2) to obtain additional information about the same antenna when it is excited otherwise than by a traveling-wave current, (3) to study the properties of a modified traveling-wave V-antenna the theoretical analysis of which is unavailable and formidable.

To avoid later confusion, a list of the symbols and notations used in the figures is provided.

E-plane pattern: the radiation pattern obtained by rotating the antenna in its plane.

H-plane pattern: the radiation pattern obtained by rotating the antenna in the plane perpendicular to the plane of the antenna.

Δ : apex angle between the two arms of the antenna.

h : length between the driving-point and the center of the loading resistor, i.e., the section with the traveling-wave current

h_T : length between the center of the loading resistor and the end of the antenna, i.e., the section with standing-wave current.

R : loading resistance

θ : angle between the direction of the incident wave and the line bisecting the antenna in the H plane. $\theta = 0$ when the line bisecting the apex angle points toward the transmitting antenna.

ϕ : the same as above but in the E plane. $\phi = 0$ when the line bisecting the apex angle points toward the transmitting antenna.

There are four principal quantities to be taken as variables in the experimental study of the properties of the antenna:

(1) Loading resistance, R

(2) Apex angle of the arms, Δ

(3) Length of traveling-wave section, h

(4) Length of standing-wave section, h_T

If the experiments were to be made for five different values of each quantity with the others constant, the total number of pattern measurements to be made would be excessive. Even though the number of patterns actually measured were greatly reduced with the aid of the theoretical studies described in a separate report, it would, nevertheless, be somewhat overwhelming to attempt to present them all in one report. Consequently, only typical measured curves which are essential to the formulation of general descriptive statements from all of the available experimental data are included.

6. EFFECTS OF THE LOADING RESISTANCE

As the loading resistance deviates from the optimum (which is determined by the length and the apex angle) for exciting the antenna predominantly with a traveling wave, the distribution of current becomes a standing wave. As a consequence, the overall picture of the patterns both in the E and H planes changes significantly.

To start with, the resistance of the loading carbon-film resistors was measured at 600 Mc/s by inserting it in a coaxial line at one-half wavelength from the short-circuited end as shown in Fig. 7. The measurement of the position of the standing-wave current (or voltage) minimum and the standing-wave ratio determined the impedance of the resistor. With six resistors measured, the real part of the impedance indicated that the resistance is close to the values specified by the manufacturer with errors ranging from zero to ten percent. However, the significant imaginary part of the impedance indicated that the resistors are capacitive.

This unwanted capacitance can be compensated for by using the electrical center of the resistor instead of its physical center in designing the dimensions of the traveling-wave V-antenna. The distance between the electrical center and physical center can be obtained by determining the distance between the position of the physical center and that of the nearest voltage minimum where the impedance is real. The measured distance between the electrical and physical centers ranged from 0.01λ to 0.05λ .

Four resistances, R = 150, 200, 250, and ∞ ohms were used throughout the measurements, unless otherwise specified. The infinite resistance was an air space of the same length as the other resistors.

Figure 8(a) and (b) through 10 (a) and (b), are the measured field patterns which illustrate the effects on the radiation patterns of the variation of resistance with other quantities kept constant.

The figures 8 (a) - 10 (a) are E-plane patterns, 8 (b) - 10 (b) H-plane patterns. They are for antennas with $h = \lambda/2$ and $\Delta = 90^\circ$ in Figs. 8 (a) and (b); $h = \lambda$ and $\Delta = 60^\circ$ in Figs. 9 (a) and (b) ; $h = 7/4\lambda$ and $\Delta = 60^\circ$ in Figs. 10 (a) and (b). In all cases the end section is $h_T = \lambda/4$. These are the patterns of the antenna with the combinations of h and Δ that yield results closest to those theoretically determined for minimum beam width. It is observed in the figures that while the beam widths of the patterns in the E plane are significantly affected by the changes in the loading resistance, those in the H plane are insensitive to the values of R and the beam width varies by no more than 5° throughout the range of resistance.

The front-to-back ratio is defined as the ratio of the intensity in the direction $\phi = 180^\circ$ ($\theta = 180^\circ$) to that in the direction $\phi = 0^\circ$ ($\theta = 0^\circ$) in the E plane (H plane). The front-to-back ratio of the traveling-wave V-antenna is larger than that of the standing-wave V-antenna by as much as 4 to 7 dB depending upon the loading resistor. (Note that the pattern with $R = \infty$ can be considered as that of a standing-wave V-antenna with added collinear end

sections of length $h_T = \lambda/4$. As a matter of fact, the contribution to the pattern from these parasitic collinear sections is insignificant because the length is far from resonance and the amplitude of the induced current is very small. As the loading resistance deviates from the optimum value, the excitation is by both the incident and growing reflected wave. The pattern then tends to become bidirectional and the front-to-back ratio, in general, decreases.

All of the patterns shown in Figs. 8 through 10 have the largest front-to-back ratio when R = 250 ohms. However, measured patterns which were not included to conserve space showed that resistances smaller than this value actually gave the largest front-to-back ratio for antennas with longer arms and smaller apex angles.

It is also to be noted that the longer the antenna, the less critical the value of the resistance is in its effect on the radiation patterns in both E and H planes.

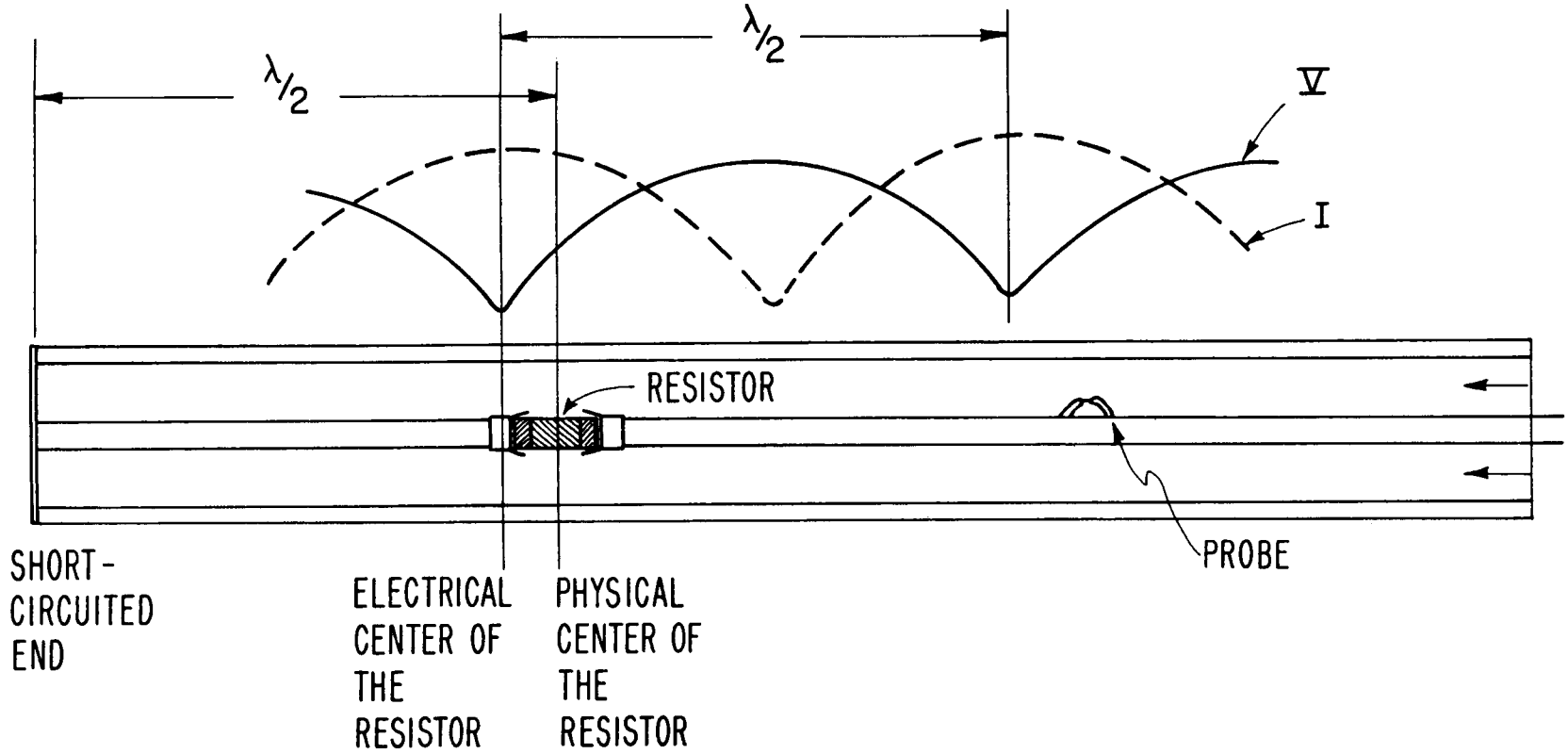

FIG. 7 DETERMINATION OF THE ELECTRICAL CENTER OF THE LOADING RESISTORS.

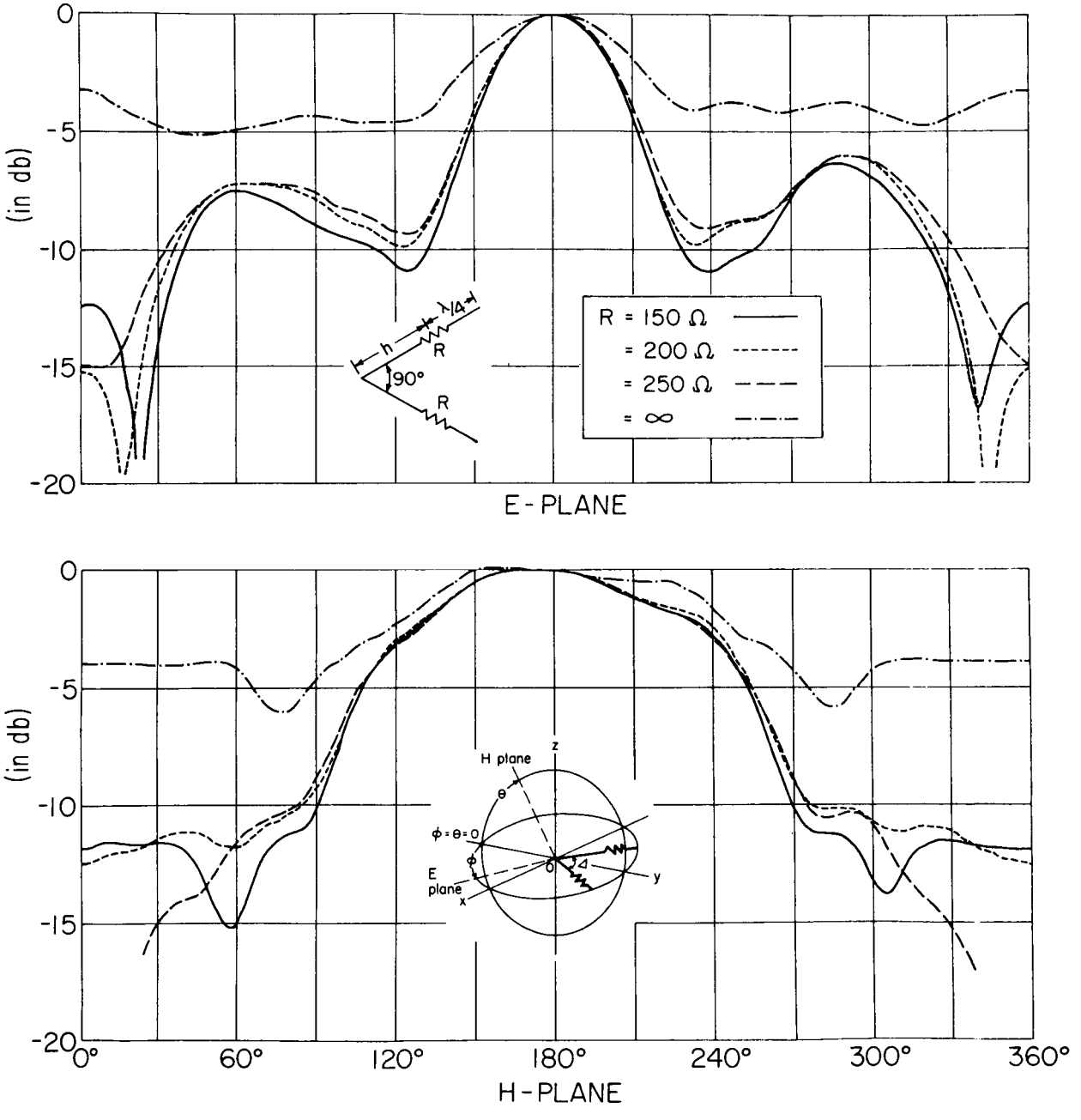

FIG. 8 EFFECT OF THE LOADING RESISTANCE ON THE RADIATION PATTERN OF THE ANTENNA WITH $h = \lambda/2$, $h_T = \lambda/4$, AND $\Delta = 90°$.

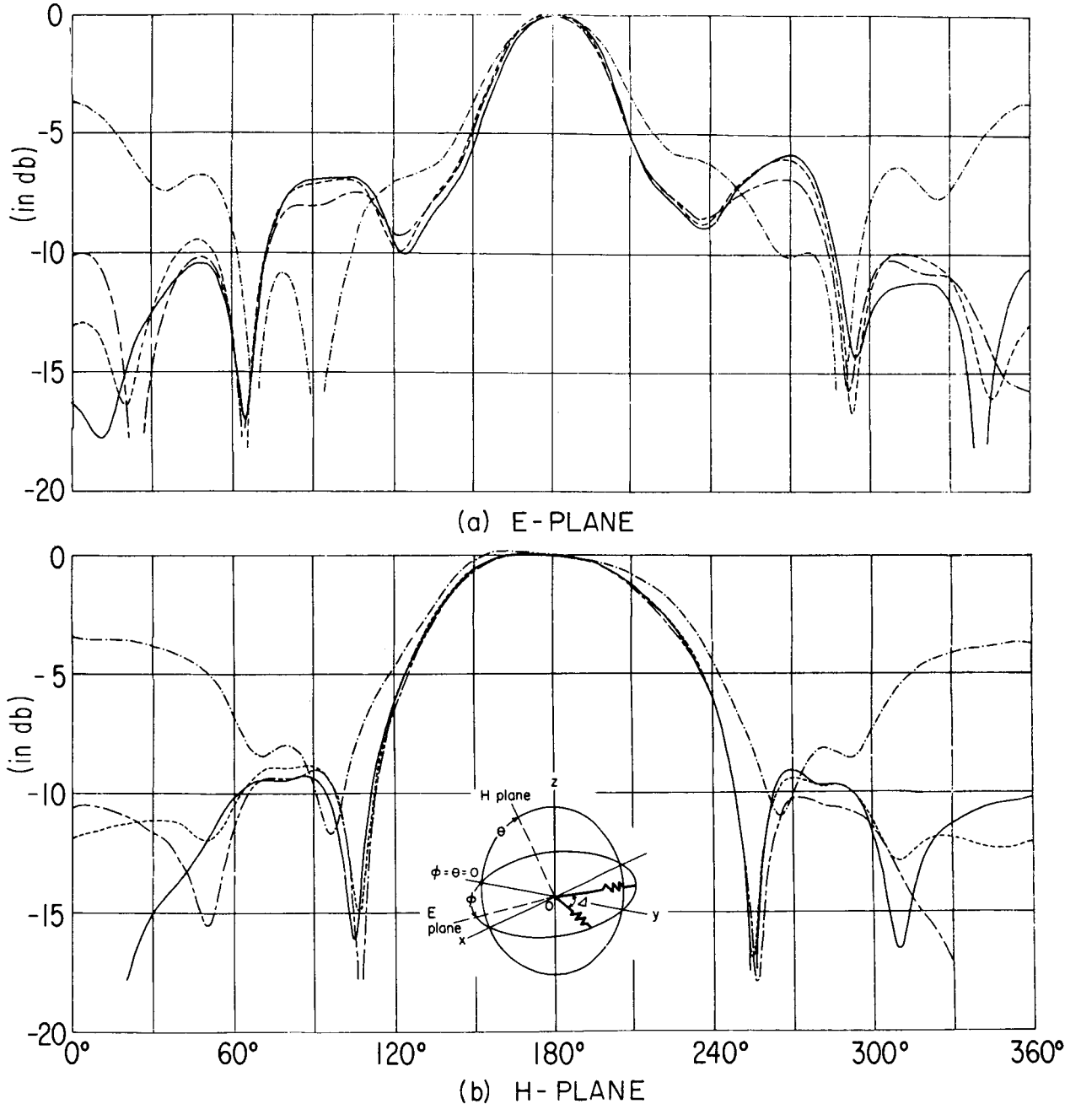

FIG. 9 EFFECT OF THE LOADING RESISTANCE ON THE RADIATION PATTERN OF THE ANTENNA WITH $h = \lambda$, $h_T = \lambda/4$, AND $\Delta = 60°$.

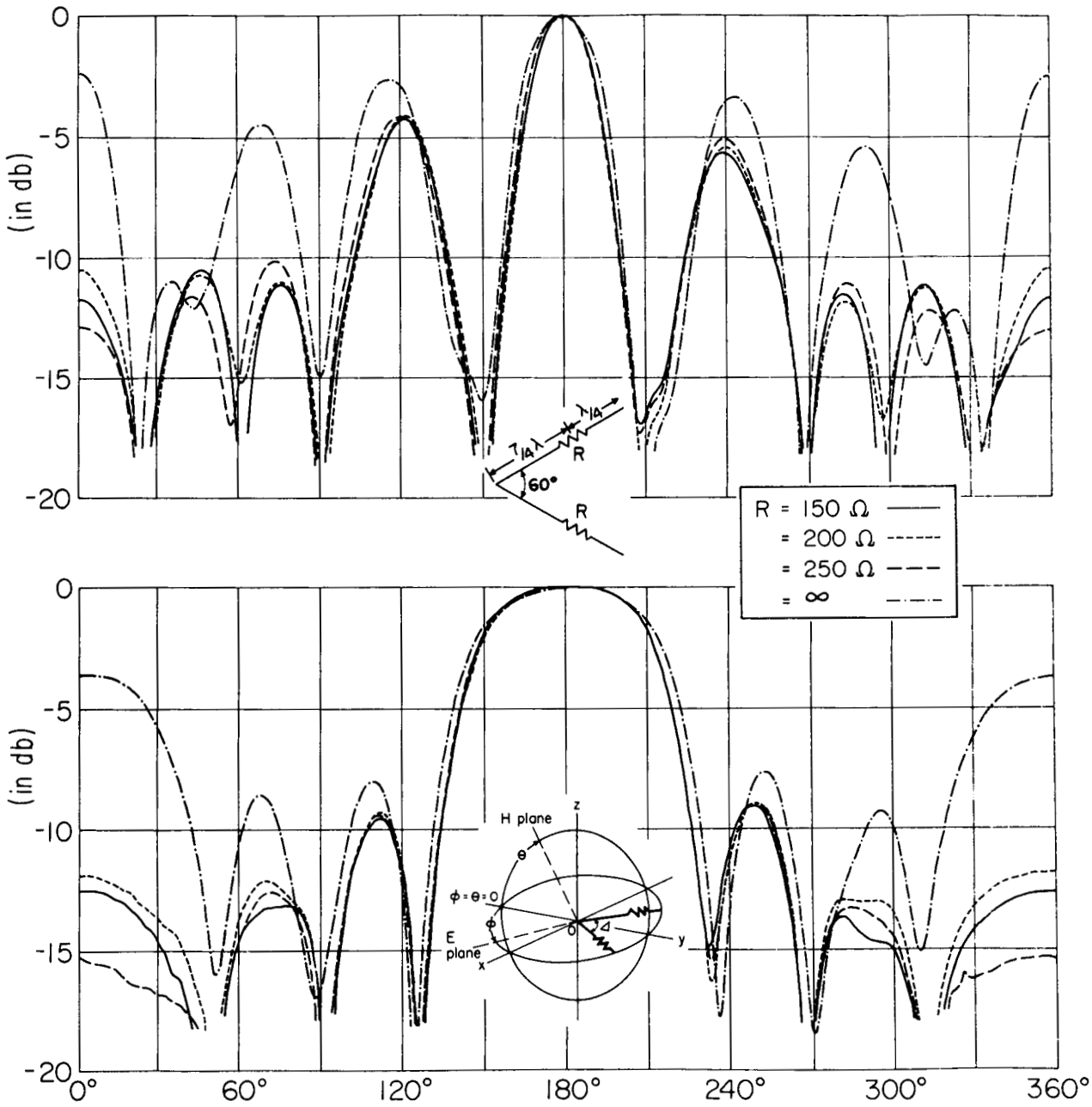

FIG. 10 EFFECT OF THE LOADING RESISTANCE ON THE RADIATION PATTERN OF THE ANTENNA WITH $h = 7/4\ \lambda$, $h_T = \lambda/4$, AND $\Delta = 60°$ IN E-PLANE

7. EFFECTS OF THE LENGTH OF THE ANTENNA

In this series of measurements the electrical length of the antenna was used as the variable. The measured radiation patterns of the antenna for the range $h = \lambda/2$ to 10λ with $\Delta = 60^{\circ}$ and $R = 250$ ohms in Figs. 11 (a) and (b) and with $\Delta = 90^{\circ}$ and $R = 250$ ohms in Figs. 11 (a) and (b). As before, the figures (a) are E-plane patterns, and the figures (b), H-plane patterns. The beam width of the major lobe, in general, decreases (the rigorous statement requires a consideration of the apex angle which will be discussed in the next section),and the number of side lobes and their height increase when the length of the antenna is increased.

The radiation patterns in the H planes are less sensitive to the length of the antenna than those in the E plane.

With larger antennas the difference between the patterns for traveling-wave and standing-wave excitations is less than with shorter antennas. Note also that the choice of the apex angle is much more critical in its effect on the patterns with longer antennas than with shorter ones.

In the theoretical studies the mathematical expression for the field pattern becomes much simpler, if the contribution from the standing-wave current at the end sections is assumed to be negligible. It is, therefore, interesting to know quantitatively how significant is the contribution from the standing-wave current in these sections. Measurements of the radiation pattern were repeated with the end sections bent to be perpendicular to the plane of the antenna (see Fig. 13), and with the sections straight. The differencesin the measured radiation patterns are the contributions from the end sections.

In Figs. 13 (a), (b), both E- and H-plane patterns of the antenna with $h = \lambda$, $h_T = \lambda/4$, and $R = 250$ ohms are shown with the apex angle Δ. It is seen that the contribution by the end sections does not alter the shape of the main lobes in both E and H planes, but the first nulls are deeper with the end sections bent up as expected. The front-to-back ratio is smaller with the bent end sections which contradicts the expectation that the front-to-back ratio is larger because of the absence of the contribution of the standing wave (or bidirectional wave) in the end section. The decrease in the back-to-front ratio may have been mainly due to the generation of the reflected waves due to the bend.

With the measurements described so far, the resistor was at a current maximum one-quarter wavelength from the end of the antenna. This is desirable in exciting the antenna predominantly by a traveling-wave current.

With reference to the frequency sensitivity of the radiation pattern of the traveling-wave V-antenna, however, it is clear that as the frequency is changed the resistor does not remain a quarter wavelength from the end, so that a shift to a more standing-wave type of excitation occurs. This shift is primarily responsible for the frequency sensitivity of the radiation pattern. The change in the length of the antenna arms in terms of the wavelength is of secondary significance. This statement was verified experimentally by repeating the pattern measurements of the antenna with $h = \lambda$, $\Delta = 60^{\circ}$, $R = 250$ but with successively shorter end sections. The measured patterns in both E and H planes are shown in Fig. 14 (a) and (b). It is seen from the figure that with a decrease in h_T from $h_T = \lambda/4$ the front-to-back ratio is decreased by as much as 9 dB . This gives a clear indication of the increase in the standing wave along the entire antenna. It is noteworthy that the shape of the main lobe is rather insensitive to changes in the length of the end sections.

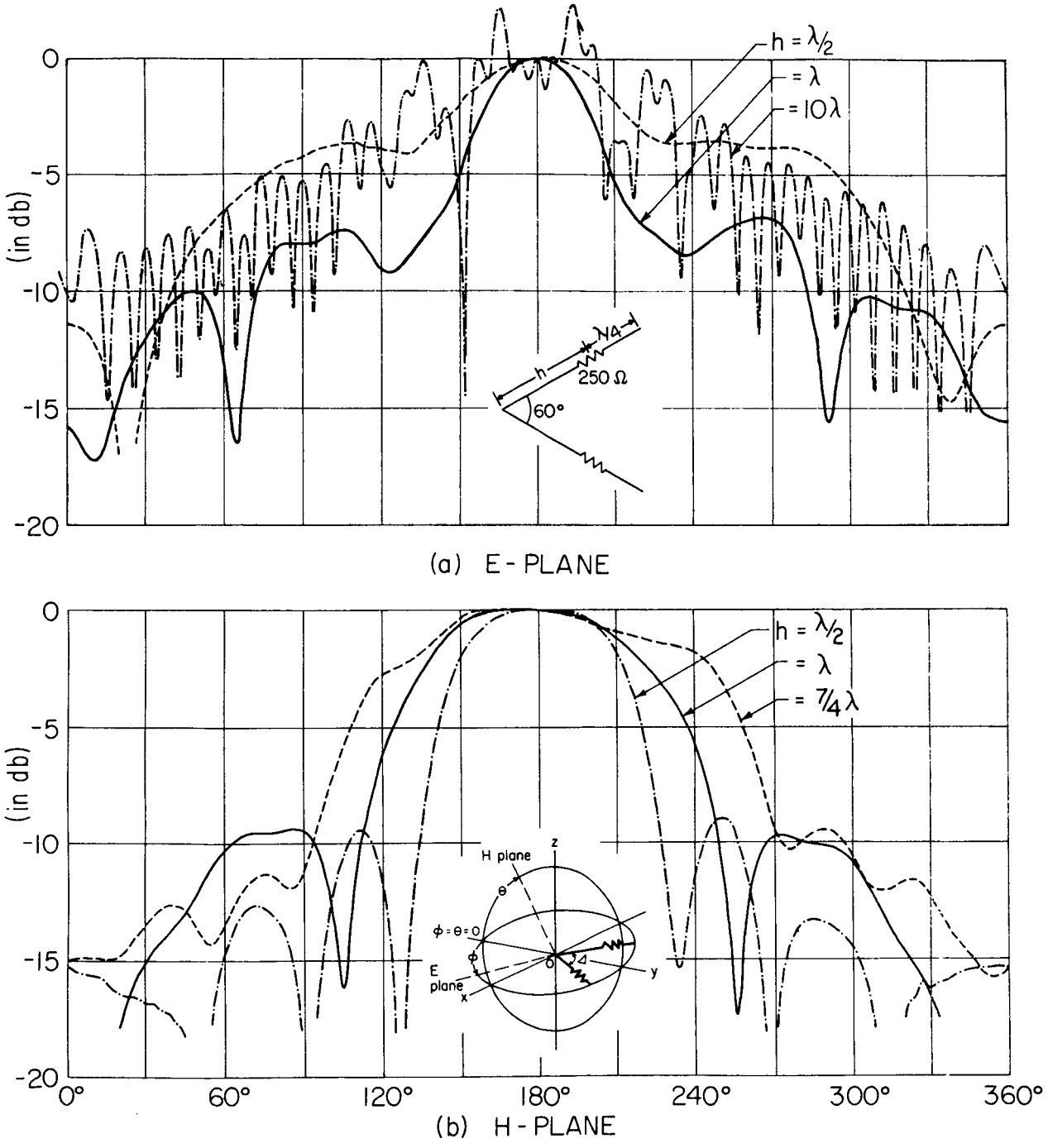

FIG. 11 EFFECT OF THE LENGTH ON THE RADIATION PATTERN OF THE ANTENNA WITH $\Delta = 60°$ AND $R = 250$ OHMS $h_T = \lambda/4$ IN THE E-PLANE AND H-PLANE.

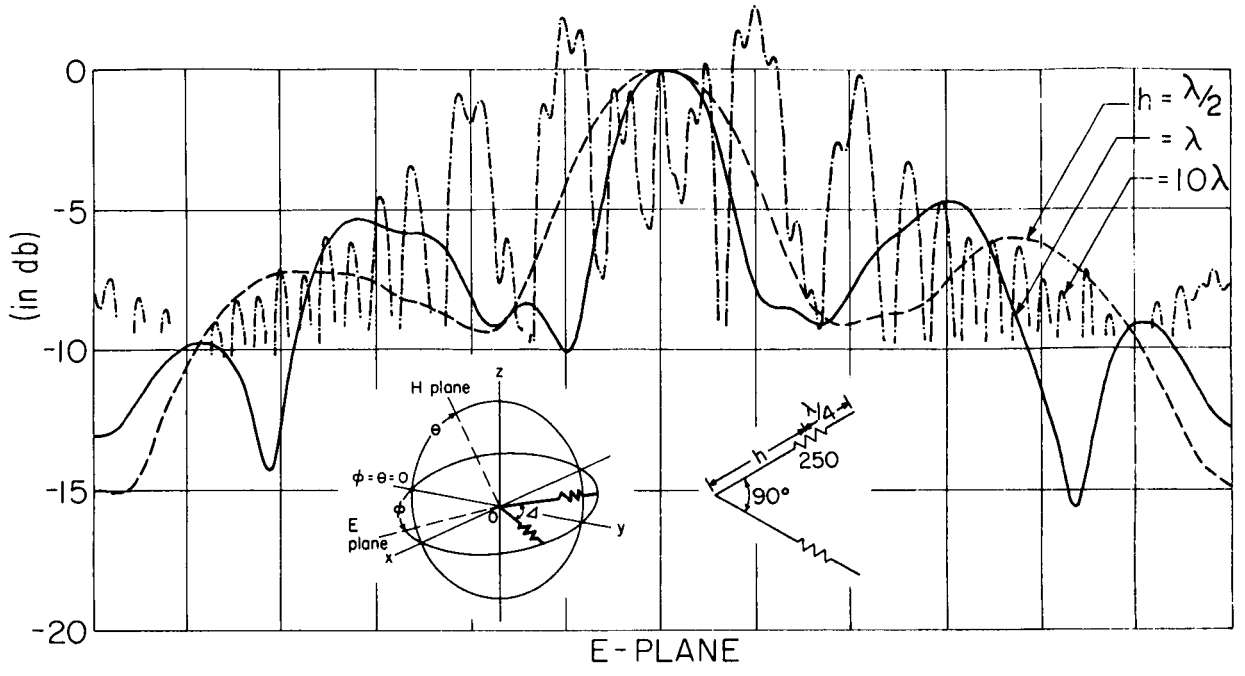

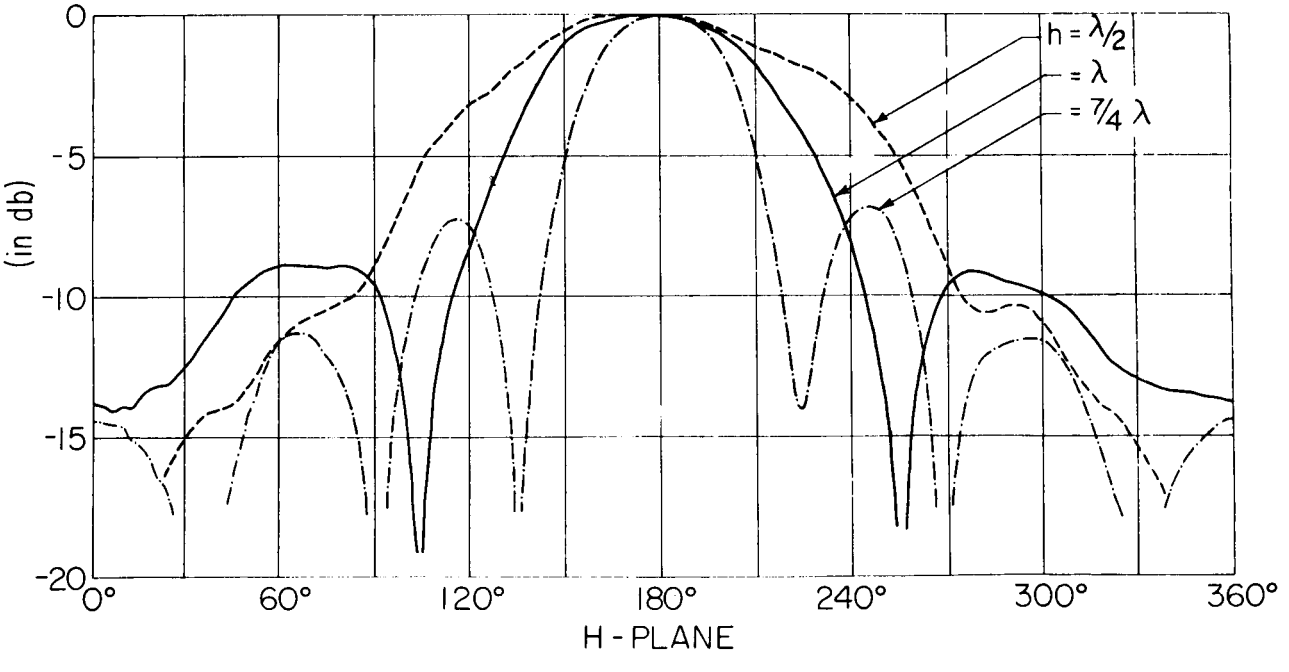

FIG. 12 LIKE FIG. 11 BUT WITH $\Delta = 90°$.

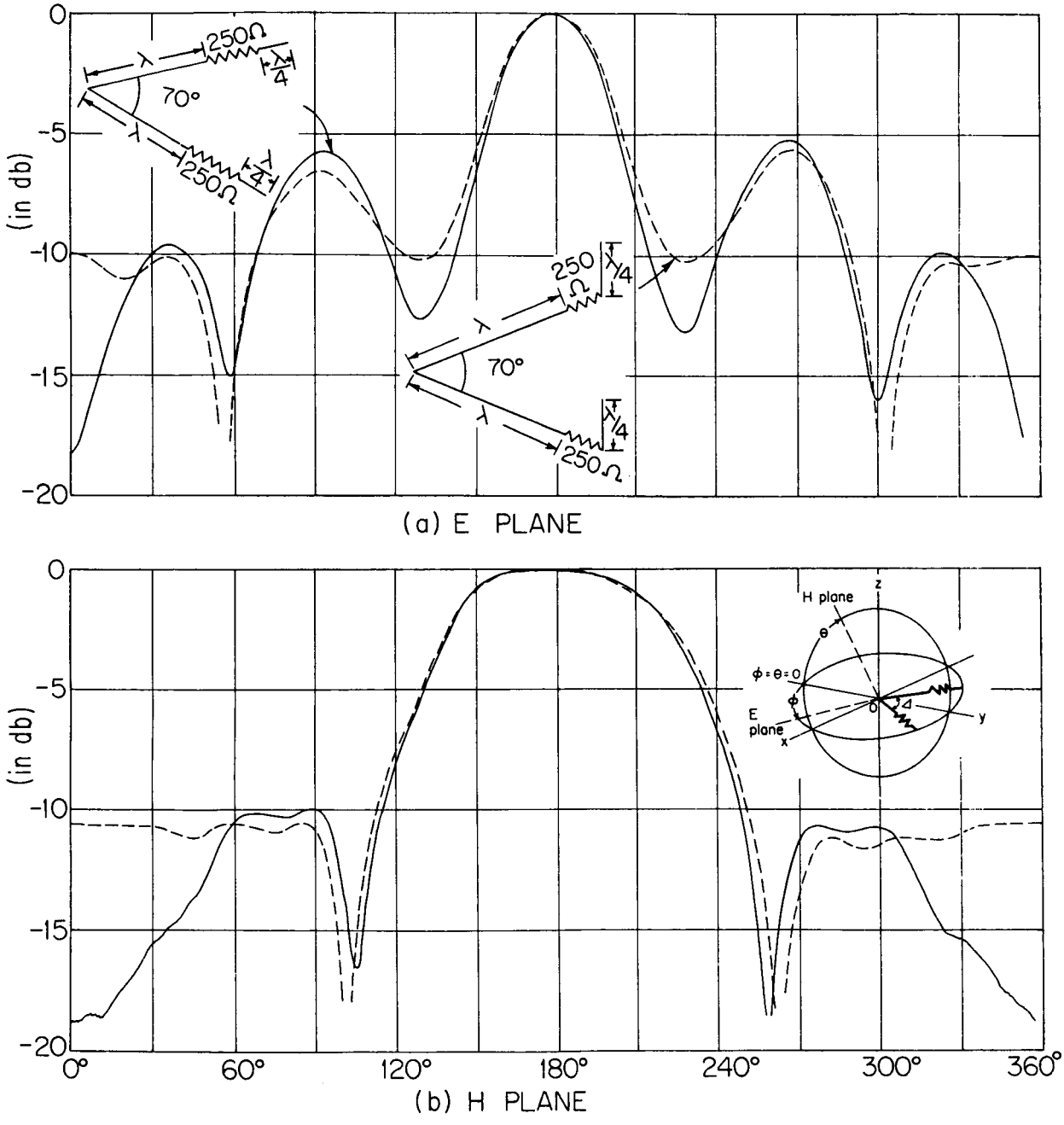

FIG. 13 RADIATION PATTERN OF THE ANTENNA WITH $h = \lambda$, $h_T = \lambda/4$, $\Delta = 70°$, R = 250 ohms WITH THE STANDING-WAVE SECTION BENT AT RIGHT ANGLES AND STRAIGHT.

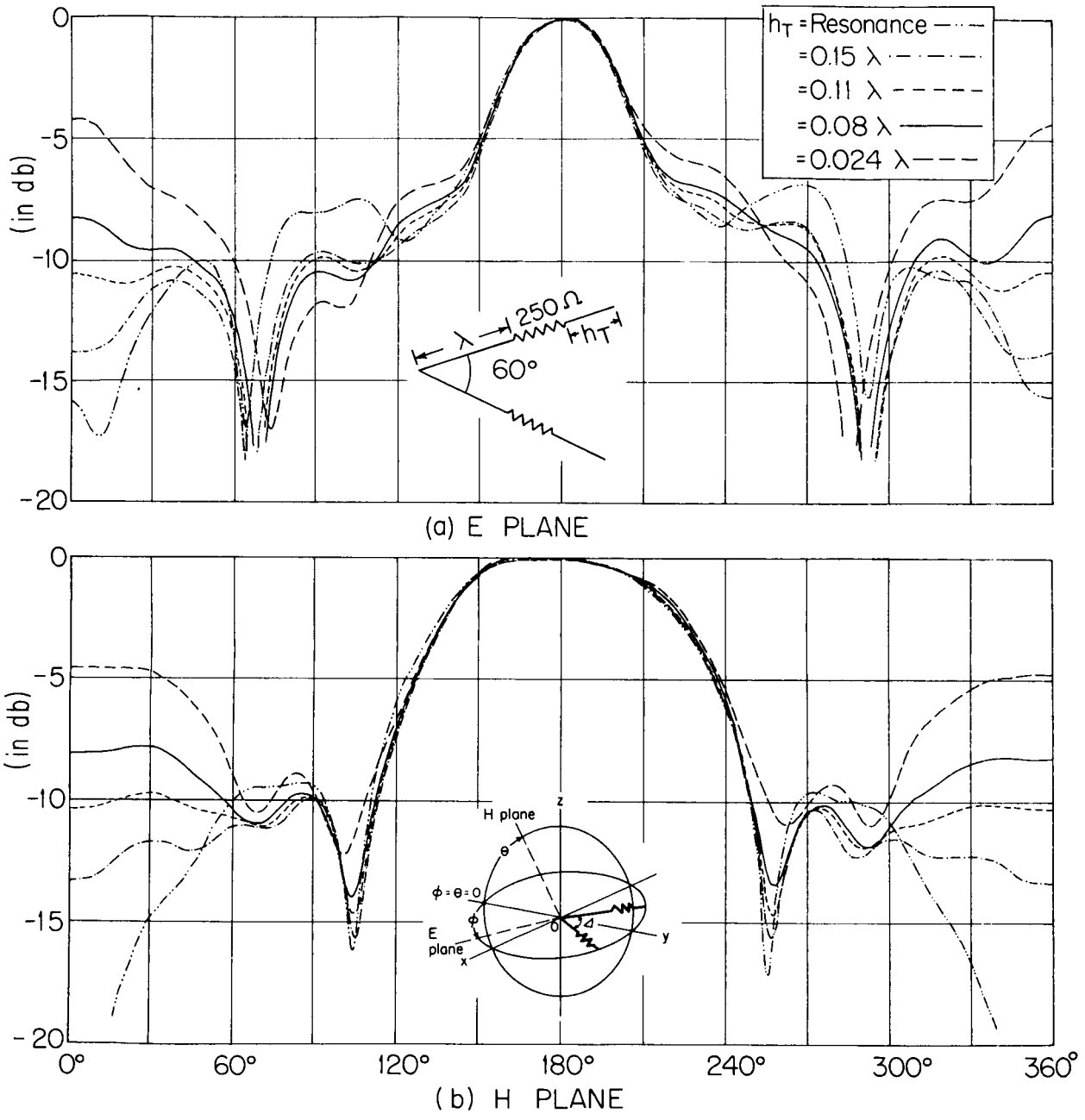

FIG. 14 RADIATION PATTERNS OF THE ANTENNA WITH $h = \lambda$, $\Delta = 60°$, AND $R = 250\,\Omega$ TAKING THE LENGTH OF THE END SECTION h_T AS A VARIABLE.

8. EFFECTS OF THE APEX ANGLE OF THE ANTENNA

The radiation patterns of antennas with four different lengths were measured at small intervals in the apex angle Δ. They are shown in Figs. 15 through 18. The parameters used in each figure are tabulated as follows:

Patterns in the E Plane

	h/λ	R	h_T	Δ
Fig. 15(a)	1/2	250	$\lambda/4$	$10^\circ, 20^\circ, 35^\circ, 45^\circ$
(a')	"	"	"	$60^\circ, 70^\circ, 83^\circ, 90^\circ, 180^\circ$
Fig. 16(a)	1	"	"	$10^\circ, 20^\circ, 35^\circ, 45^\circ$
(a')	"	"	"	$60^\circ, 70^\circ, 83^\circ, 90^\circ, 180^\circ$
Fig. 17(a)	7/4	"	"	$10^\circ, 35^\circ, 60^\circ$
(a')	"	"	"	$70^\circ, 83^\circ, 90^\circ, 180^\circ$
Fig. 18(a)	10	"	"	$10^\circ, 20^\circ, 35^\circ$
(a')	"	"	"	$60^\circ, 70^\circ, 83^\circ$

Patterns in the H Plane

	h/λ	R	h_T	Δ
Fig. 15(b)	1/2	250	$\lambda/4$	$35^\circ, 60^\circ, 90^\circ$
Fig. 16(b)	1	"	"	$35^\circ, 60^\circ, 90^\circ$
Fig. 17(b)	7/4	"	"	$35^\circ, 60^\circ, 90^\circ$

The radiation pattern of the traveling-wave V-antenna is a superposition of the radiation patterns of each arm excited by a wave traveling from the driving point to the end. Hence, the radiation pattern has the narrowest beam width when the apex angle is so arranged that the direction of the major lobe of the field pattern of the current in one of the arms along the antenna overlaps with that of the other. The mathematical expression for the field pattern of the traveling-wave current in one of the arms is given by the integral

$$E_\theta = \frac{j\omega\mu}{4\pi} \int_0^h I_o e^{-j\beta z} e^{j\beta z \cos\theta} \sin\theta \, dz \qquad (1)$$

and the theoretical optimum apex angle is identical with the angle of the major lobe of Eq. (1).

It is, therefore, interesting to list the apex angles which give the narrowest beam width for several lengths of antenna measured, and to compare these with the respective beam widths. Table I shows a list of these quantities. In column I, are shown one-half of the apex angles actually measured together with the theoretical optimum apex angle (angle for the narrowest beam width) in parentheses; in column II, is one-half of the beam width; and in column III, the theoretical beam width for the corresponding apex angle. An excellent agreement between the theoretical and experimental results is observed for antennas of shorter length.

TABLE I

Theoretical and experimental beam width with respect to apex angle and length of antenna

	I	II	III
h/λ	$\Delta/2$ used for measurement. The numbers in parentheses are the angles of $\Delta/2$ determined theoretically to give the minimum beam width.	Half beam width (Width between $\phi = 180^\circ$ and the first minimum)	Theoretical beam width corresponding to the angles of $\Delta/2$ in the parentheses in the far left column
1/2	90° (90°)	90°	90°
1	45° (50°)	45°	45°
7/4	41.5° (38.5°)	48°	38.5°
10	10° (15°)	22°	15°

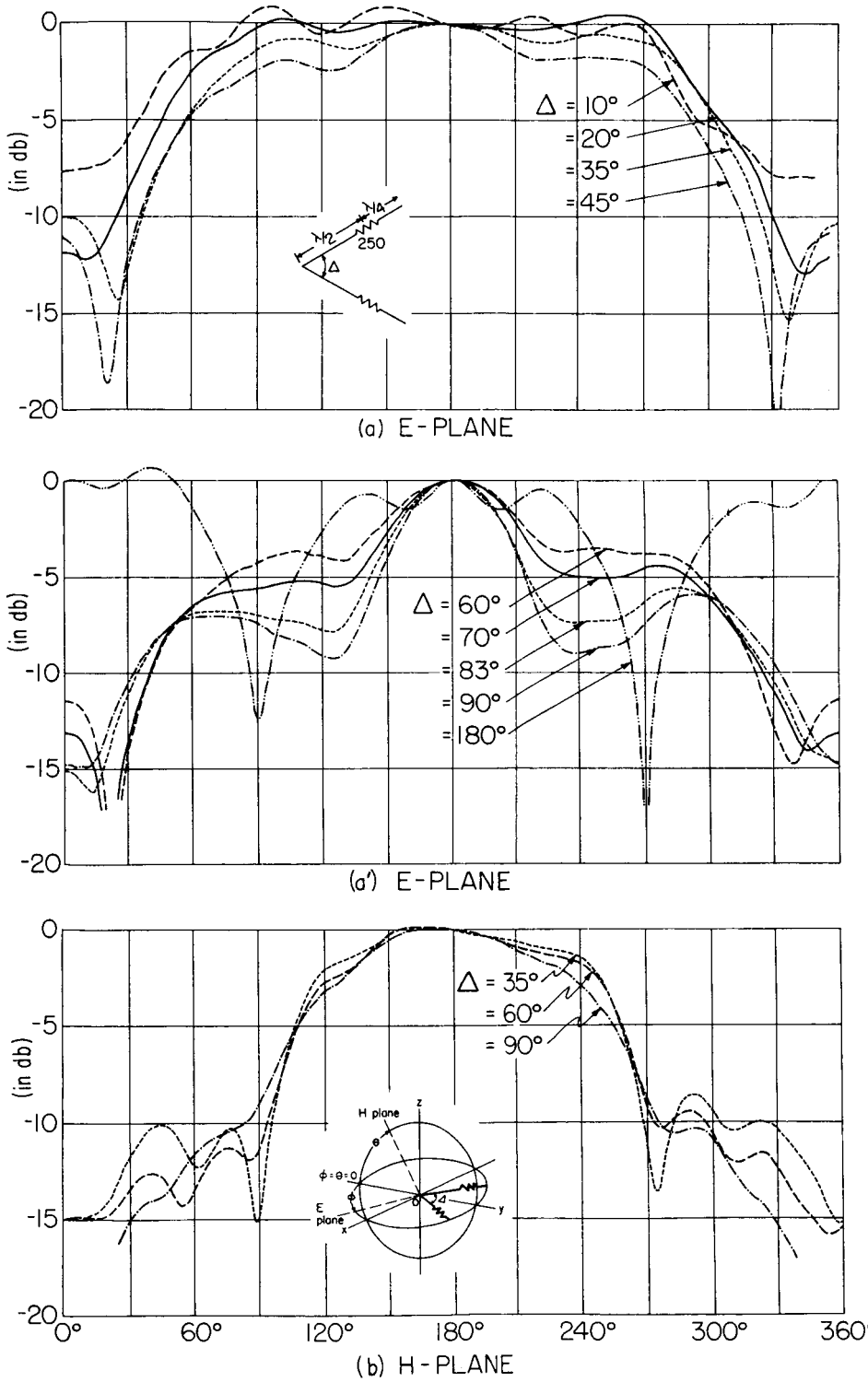

FIG. 15 RADIATION PATTERNS OF THE ANTENNA WITH $h = \lambda/2$, $h_T = \lambda/4$, R = 250 OHMS WITH THE STEPS OF THE APEX ANGLES

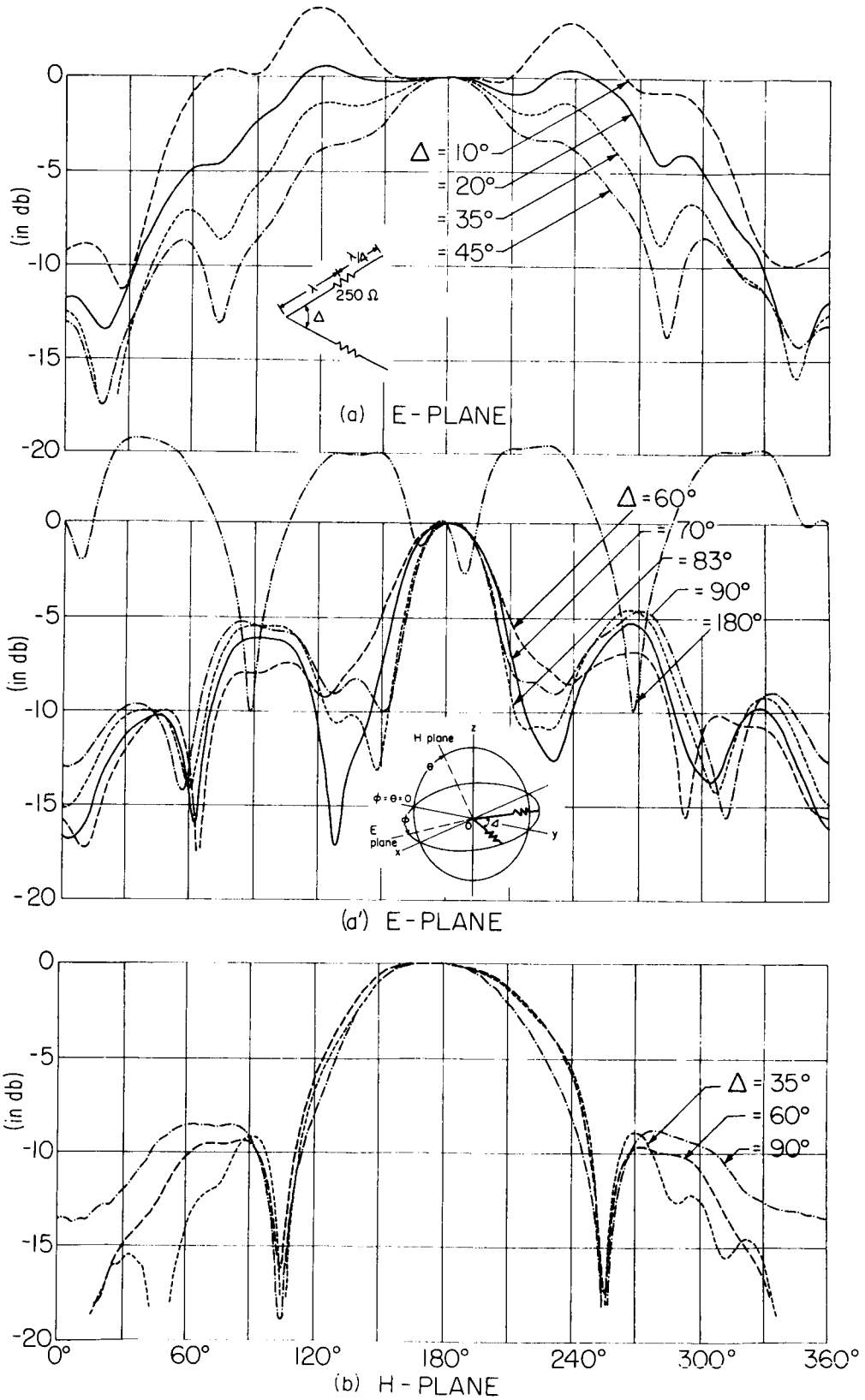

FIG. 16 LIKE FIG. 15 BUT WITH $h = \lambda$.

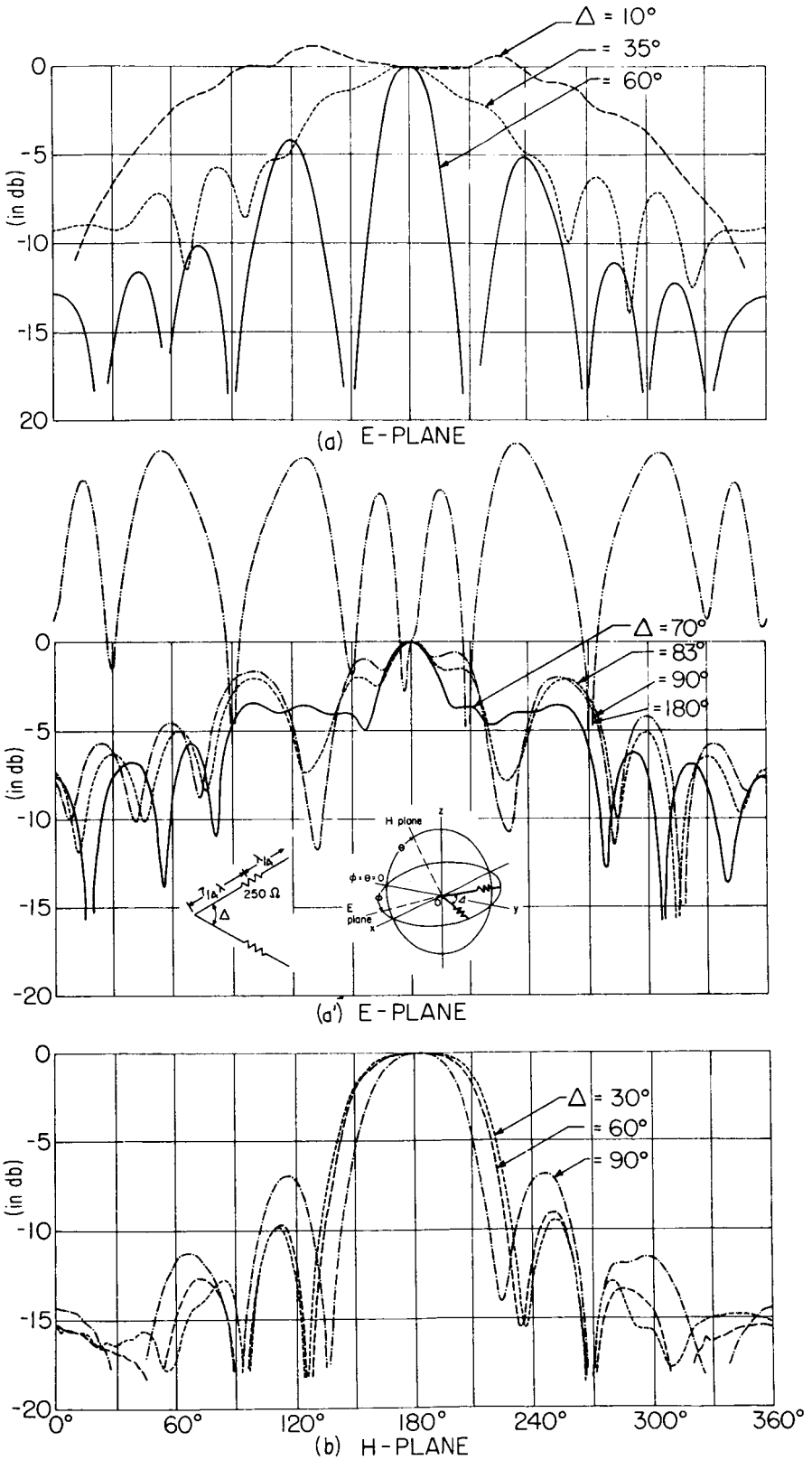

FIG. 17 LIKE FIG. 15 BUT WITH $h = 7/4\ \lambda$

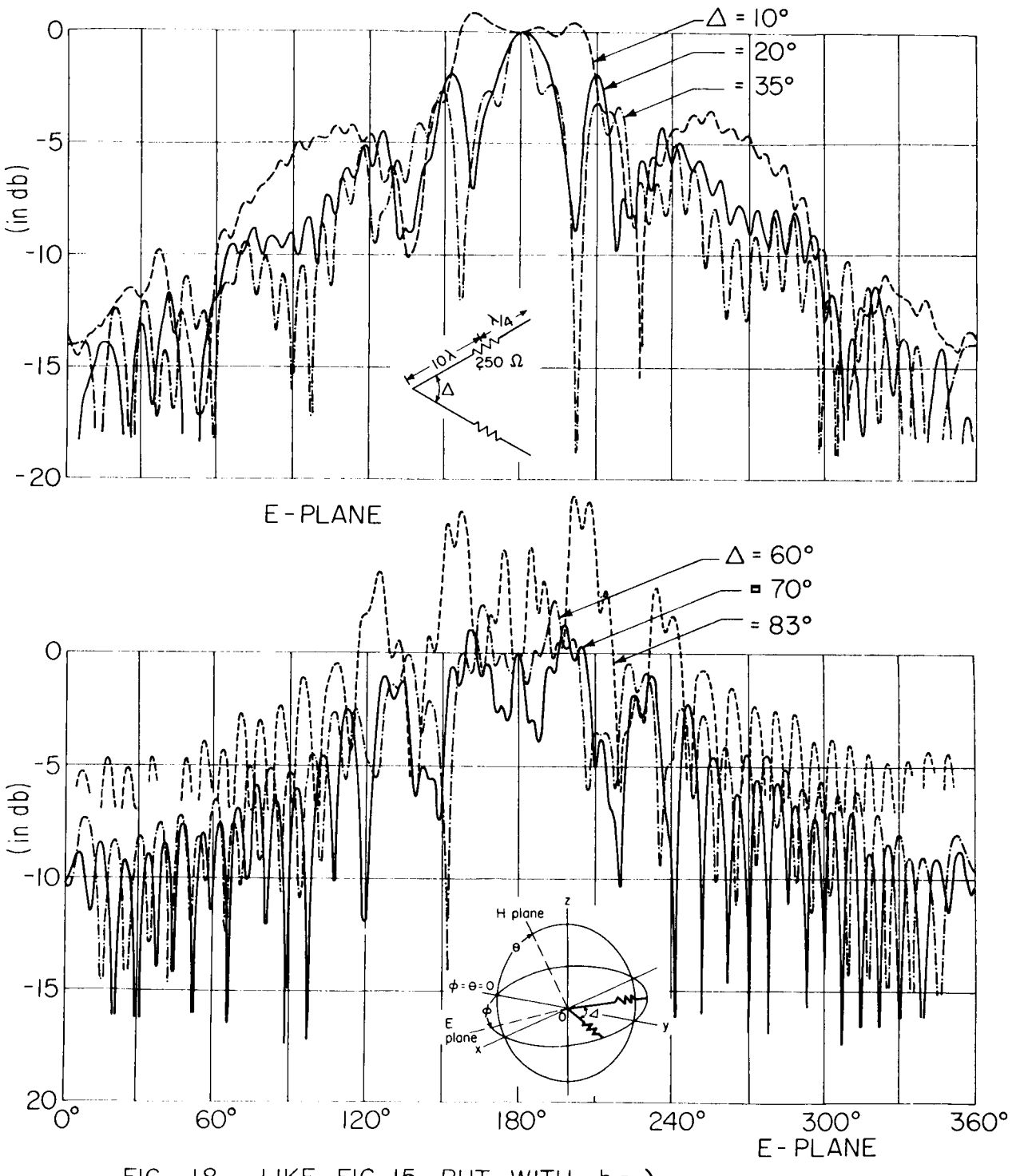

FIG. 18 LIKE FIG. 15 BUT WITH $h = \lambda$.

9. TRAVELING-WAVE V-ANTENNA LOADED WITH TWO SETS OF RESISTORS

It is the distance per wavelength from the end of the antenna to the location of the resistor that is primarily responsible for the frequency sensitivity of the radiation pattern of the traveling-wave V-antenna. For instance, if an antenna designed for operation at a frequency of f_o (see Fig. 19(a)) were operated at a frequency $2f_o$, the location of the resistor would shift to $\lambda/2$ from $\lambda/4$ away from the end (see Fig. 19(b)), resulting in the change in the impedance looking from A - A' toward T - T', and generating a reflected wave which would lead to the decrease in the front-to-back ratio of the radiation pattern.

As a traveling-wave V-antenna of improved type, an antenna loaded with two resistors with proper spacing between them, was tested. The dimensions of the antenna are shown in Fig. 19(c). Such an antenna can be operated properly both at the frequency f_o and at the frequency $2f_o$ with somewhat reduced qualities.

Figure 20(a) shows the measured E-plane patterns of the antennas whose dimensions are represented by Fig. 19(c) which corresponds to the operation of the doubly-loaded antenna at the frequency, f_o.

Figure 20(b) shows the measured E-plane patterns of the antenna whose dimensions are represented by Fig. 19(d) which corresponds to the operation of the same antenna at the frequency $2f_o$. Note that only a slight decrease in the front-to-back ratio was observed in the patterns in Fig. 20(a) compared with those in Fig. 20(b). (The difference in the shapes of the main lobes is due to the fact that they are patterns for antennas with two different total lengths.) One of the curves shows the pattern of the antenna whose dimensions are represented by Fig. 19(b). This corresponds to the singly-loaded antenna which was originally designed for operation at a frequency of f_o, when used at the frequency $2f_o$. It is observed that this pattern has a very poor front-to-back ratio compared with the doubly-loaded antenna. Thus, the doubly-loaded traveling-wave V-antenna has frequency characteristics that are superior to those of the singly loaded antenna.

Various combinations of values of R_1 and R_2 have been tried; the results are included in Figs. 20(a) and (b). An increased front-to-back ratio was obtained by making R_1 smaller than R_2.

10. TRAVELING-WAVE V-ANTENNAS LOADED WITH PROGRESSIVELY INCREASING RESISTANCES

By loading the V-antenna with a set of resistors whose resistance is successively increased as the end is approached, the frequency sensitivity of the pattern can be significantly reduced, since there exist no definite points which separate the sections h and h_T. The progressive resistance was constructed by a series of nineteen 1/8 watt regular carbon film resistors normally used for electronic circuits (1 cm in length, 0.35 cm in diameter) with a spacing of $\lambda/40$. The dimensions of the antenna are shown in Fig. 21. The values of the resistances were determined graphically by referring to the Smith chart in Fig. 22. The impedance at the end of the antenna (see point 1 in Fig. 21) is practically infinity which can be represented by point 1, in the Smith chart. The impedance transferred to the center of the first resistor is represented by point 2, and the resistance of the first resistor represented by the distance between the points 2 and 3 is added. The impedance represented by point 3 is further transformed to the center of the resistor 2 by the same distance. The same procedure is repeated as many times as there are resistors The values of the resistances were chosen so that the locus of the impedance transformation follows the line of $R/Z_C = 1$ progressing toward the center of the Smith chart. It can be proven that such an arrangement of resistors gives a constant driving-point impedance with respect to frequency. Compare the loci 1'- 2'- 3'- at two times the previous frequency with the previous loci 1, 2, 3... . The new loci 1', 2', 3' will also follow the line of $R/Z_C = 1$ progressively toward the center of the chart, because even though the increment of the circular arc 1' - 2' is twice as long as 1-2 as a result of an increase in frequency by the factor 2, the graduations of the Smith chart near 2' and 3' are roughly twice as large as those near 2 and 3, so that the length between 2' and 3' is also twice as large as that between 2 and 3.

In Fig. 23 (a) is shown the E-plane radiation pattern of the traveling-wave V-antenna of $h = \lambda$, $\Delta = 60^\circ$ which was loaded with a series of resistors one-half wavelength long. The specifications of the resistors are shown in Fig. 21. The H-plane pattern of the same antenna is shown in Fig. 23 (b). The radiation pattern for a singly-loaded antenna (a) with a traveling-wave section of the same length, $h = \lambda$, $h_T = \lambda/4$, $R = 250$, and the radiation pattern of the antenna (b) with the series of resistors replaced by a brass tube of the same length $\lambda/2$, are also plotted in the same figure for comparison. The present antenna has a considerably narrower beam width and larger front-to-back ratio than the antennas (a) and (b).

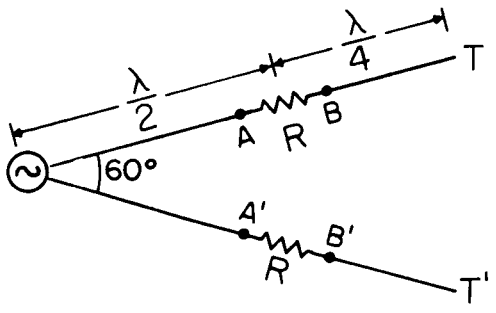

(a) MATCHED FOR FREQUENCY f_o

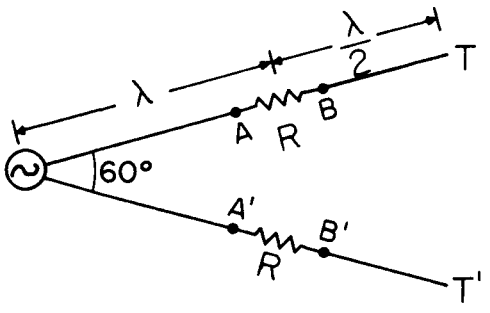

(b) THE ANTENNA WITH THE SAME PHYSICAL DIMENSION AS (a) HAS MISMATCH FOR $2f_o$

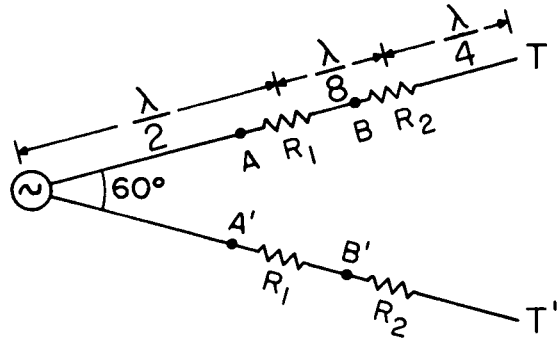

(c) DIMENSION IN WAVELENGTH OF THE DOUBLY-LOADED ANTENNA FOR f_o

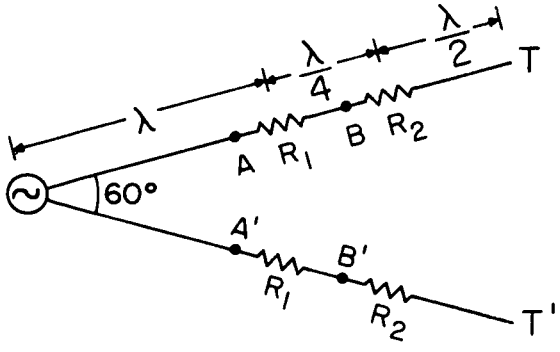

(d) DIMENSIONS IN WAVELENGTH OF THE DOUBLY-LOADED ANTENNA FOR $2f_o$

FIG. 19 DIMENSIONS OF THE TRAVELLING WAVE V ANTENNA IN TERMS OF WAVELENGTH FOR f_o AND $2f_o$.

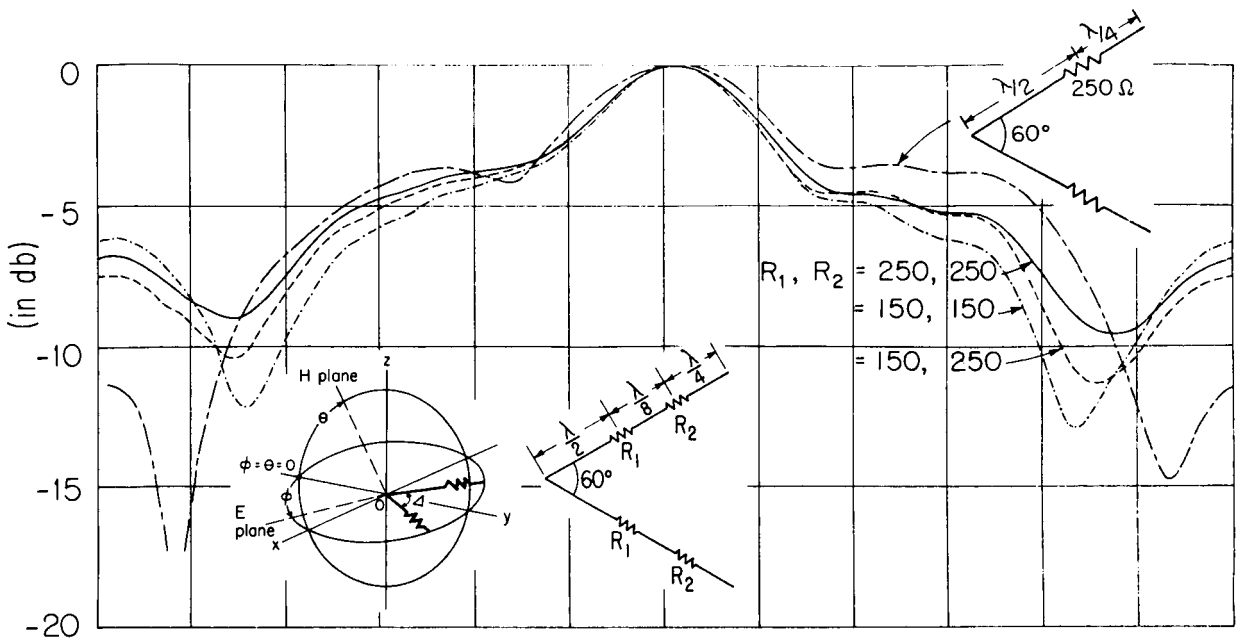

FIG. 20(a) E-PLANE RADIATION PATTERNS WITH THE DIMENSIONS SHOWN IN FIG. 19 (c)

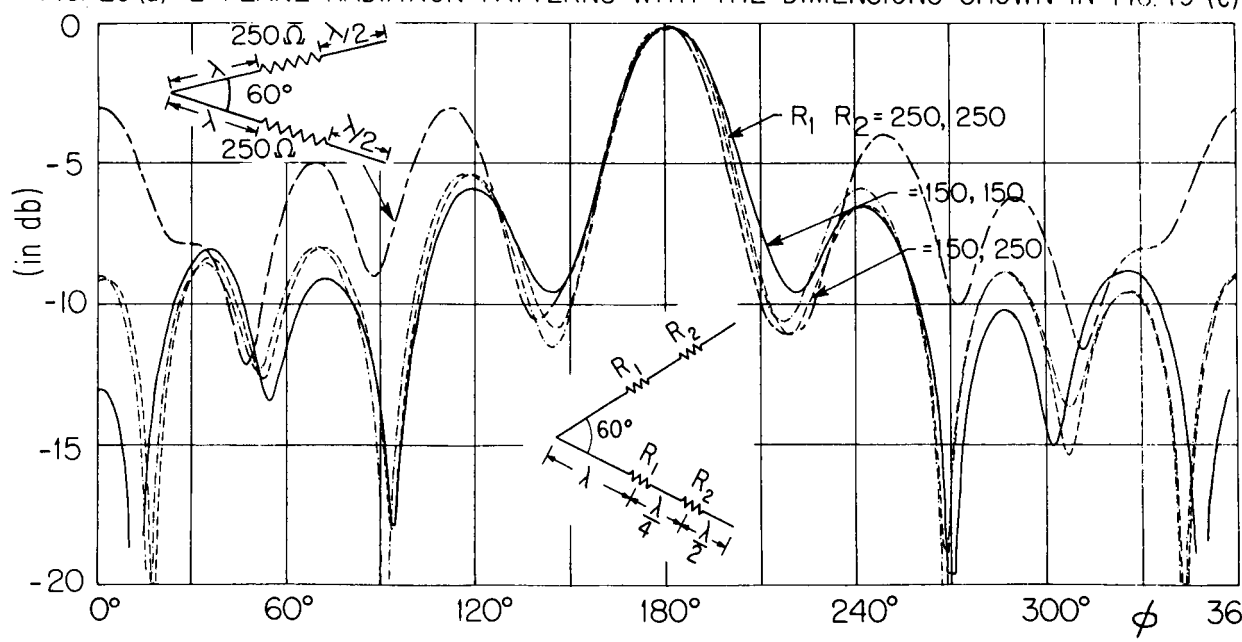

FIG. 20(b) E-PLANE RADIATION PATTERNS WITH THE DIMENSIONS SHOWN IN FIG. 19 (b) AND (d).

Values of Resistors Used: $R_1, R_2, R_3, \text{----------} R_{19}$ =

470, 220, 150, 91, 91, 75, 47, 51, 36, 47, 36, 33, 27, 24, 20,

18, 15, 12, 12.

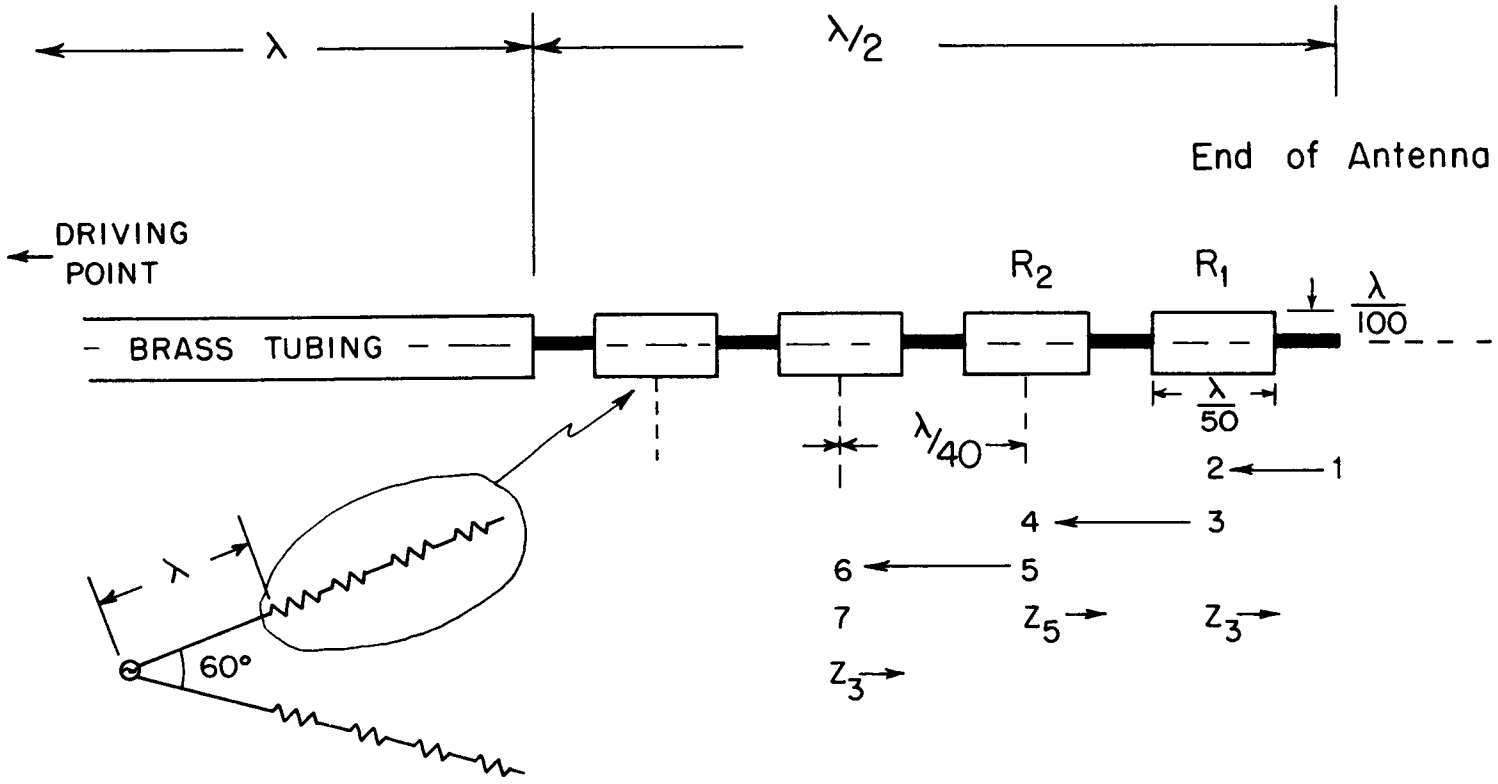

FIG. 21 DIMENSIONS OF THE LOADING RESISTOR WITH PROGRESSIVE RESISTANCE.

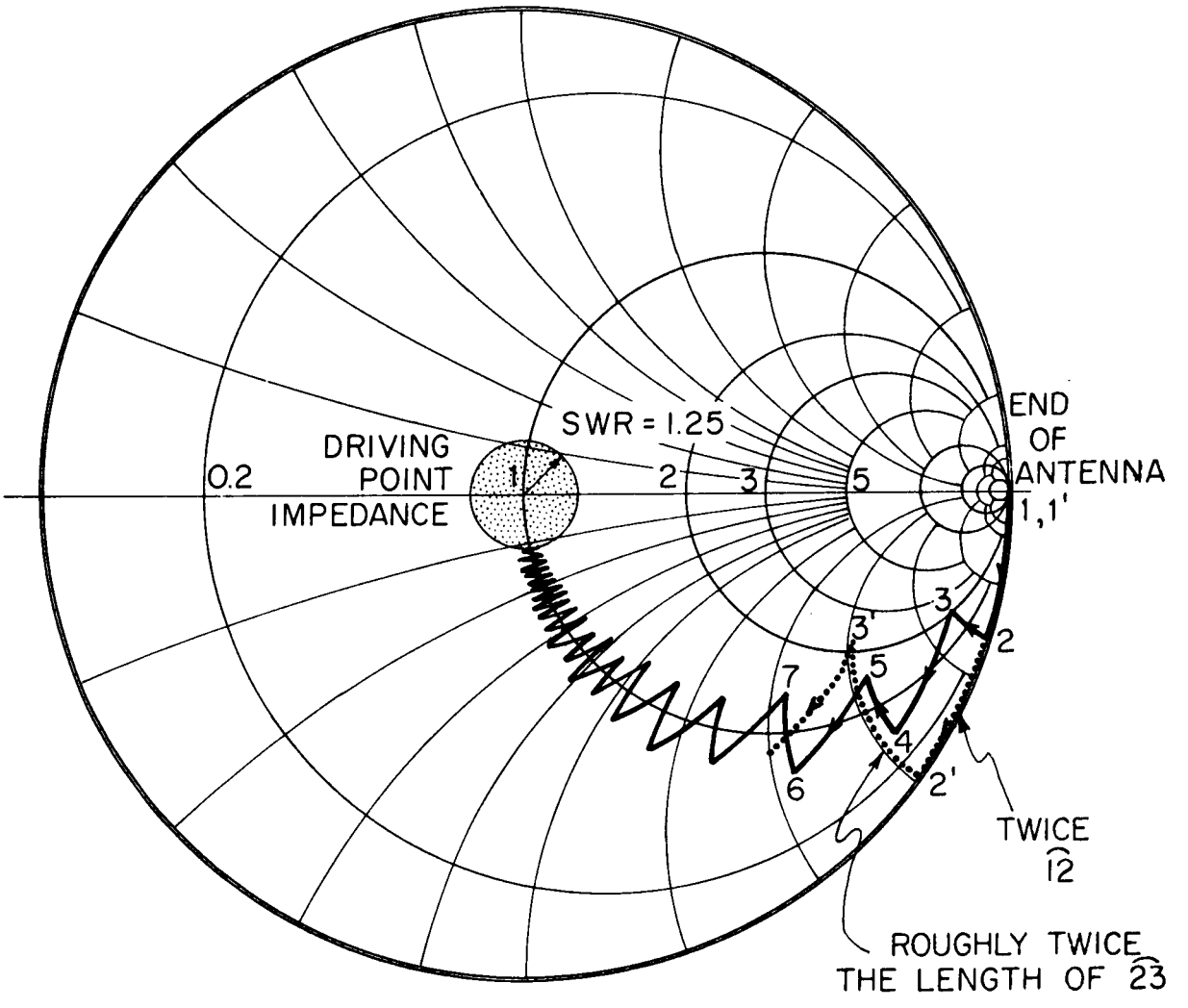

FIG. 22 LOCUS OF THE IMPEDANCE OF THE PROGRESSIVELY LOADED LINE AT TWO FREQUENCIES.

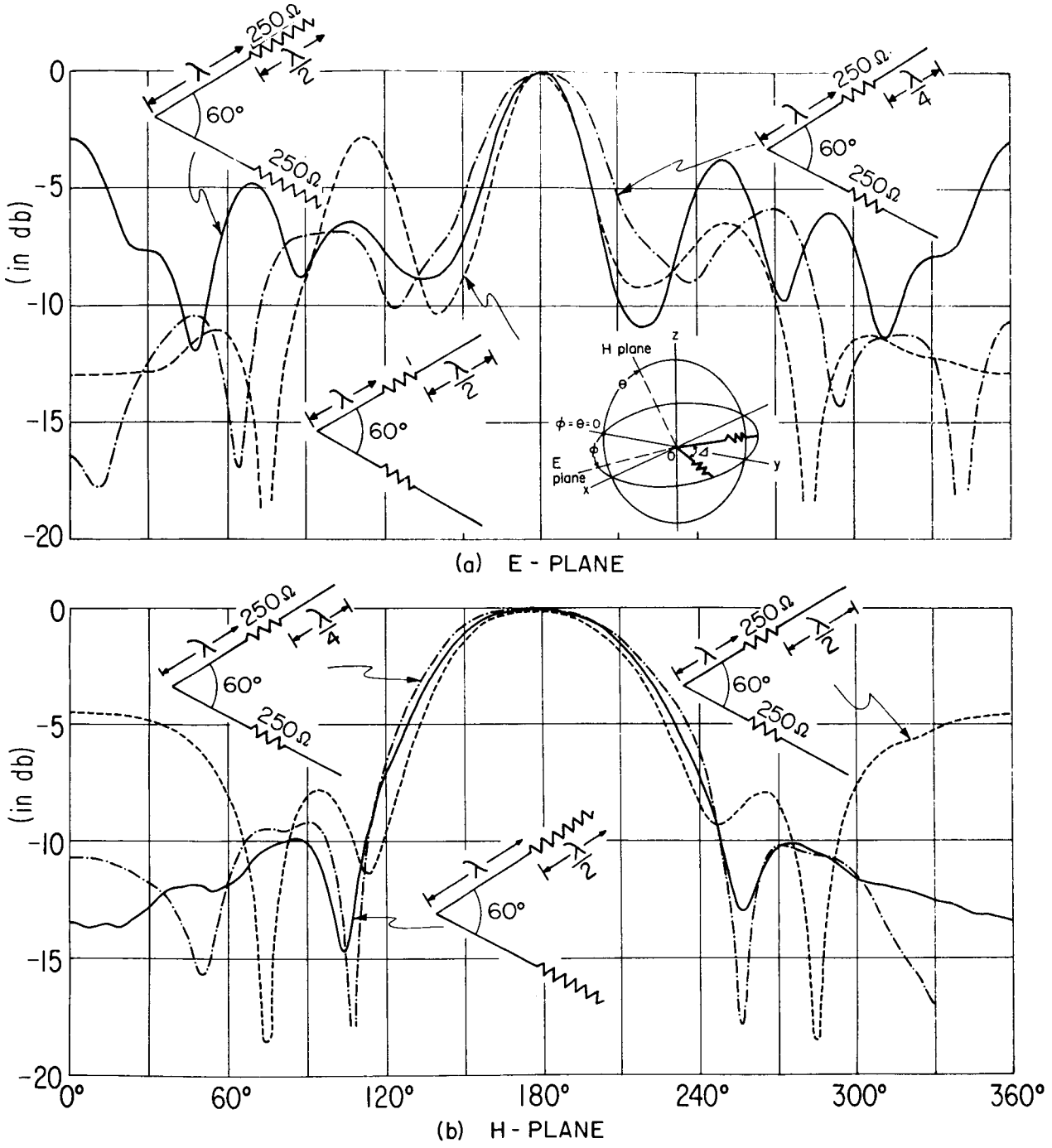

FIG. 23 RADIATION PATTERN WITH A SERIES OF RESISTORS COMPARED WITH THAT OF ONE COUPLE OF RESISTORS.

11. COMBINATIONS OF TRAVELING-WAVE V-ANTENNAS

Considerable variation in the radiation patterns can be obtained by varying the combination of the driving conditions of two sets of traveling-wave V-antennas. As shown in Fig. 24, four arms ($h = \lambda$, $h_T = \lambda/4$, $R = 250$ ohms) were placed in a plane with apex angles of 60° and 120° alternately, and either all four arms or two of them were driven with proper connections. The small circles represent the driving-point terminals in the figure. The measured radiation patterns in both E and H planes of the antenna in the six different configurations shown in Fig. 24(a) through (f) are shown in Fig. 25(a) and Fig. 25(b). Two cycles instead of one cycle of the patterns were employed for clarity.

The corresponding directions of the major lobes in Fig. 25(a) are drawn in (but not to scale) in Fig. 24. It is seen that merely by changing the connections at the driving-points, various kinds of patterns such as (a) unilateral endfire beam, (b) unilateral broadside beam, (c) bilateral endfire beam, (d) bilateral broadside beam, (e) omnidirectional beam, (f) doughnut-shaped beam. Such a variety is especially appreciated when the antenna is used for the reception of a signal whose direction of incidence is either not known or variable.

It is also noteworthy that the radiation pattern of the antenna with the configuration shown in Fig. 24(a) is very close to that of the isolated traveling-wave antenna except in the details of the minor lobes. This means that the mutual interaction of the currents in the arms is not too large and the rough prediction of the radiation pattern of the composite traveling-wave V-antenna can be made readily by superposition. It also predicts the simplicity of the adjustment of such a circularly-polarized antenna as was made up of two traveling-wave V-antennas whose planes are mutually perpendicular. This is possible because the individual adjustment of the antenna in one plane does not significantly affect the other.

12. ACKNOWLEDGMENT

The author is indebted to Professor R. W. P. King at Harvard University for his critical reading and correcting of the manuscript. Numerous helpful discussions with Trilochan Padhi are gratefully acknowledged.

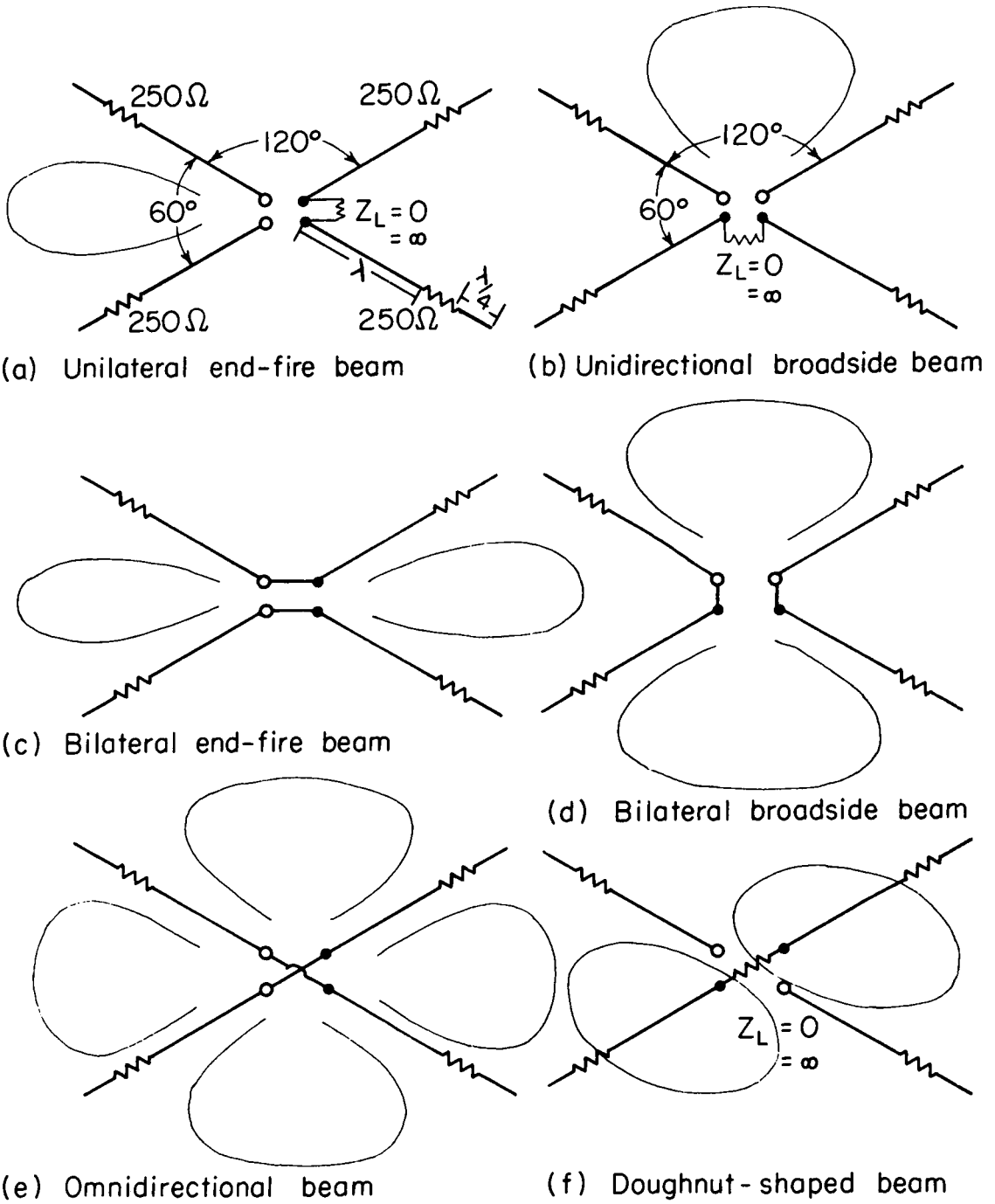

FIG. 24 VARIOUS MODES OF EXCITATION OF DOUBLE TRAVELING-WAVE V-ANTENNA AND RESPECTIVE DIRECTIONS OF THE MAJOR LOBE (NOT TO SCALE). THE SMALL CIRCLES ARE DRIVING TERMINALS. THE CORRESPONDING MEASURED RESULTS ARE SHOWN IN FIG. 26 (a) (b).

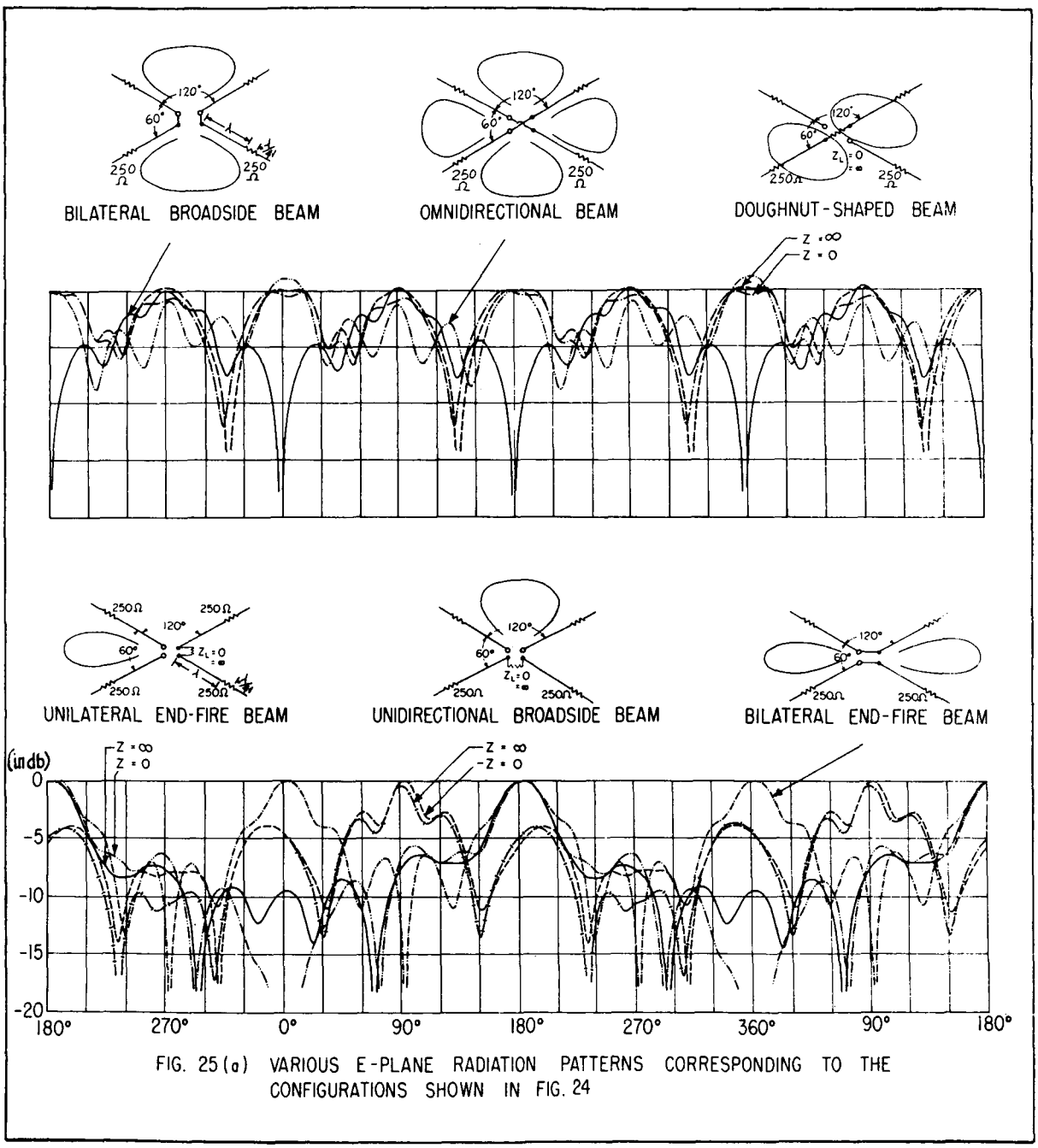

FIG. 25 (a) VARIOUS E-PLANE RADIATION PATTERNS CORRESPONDING TO THE CONFIGURATIONS SHOWN IN FIG. 24

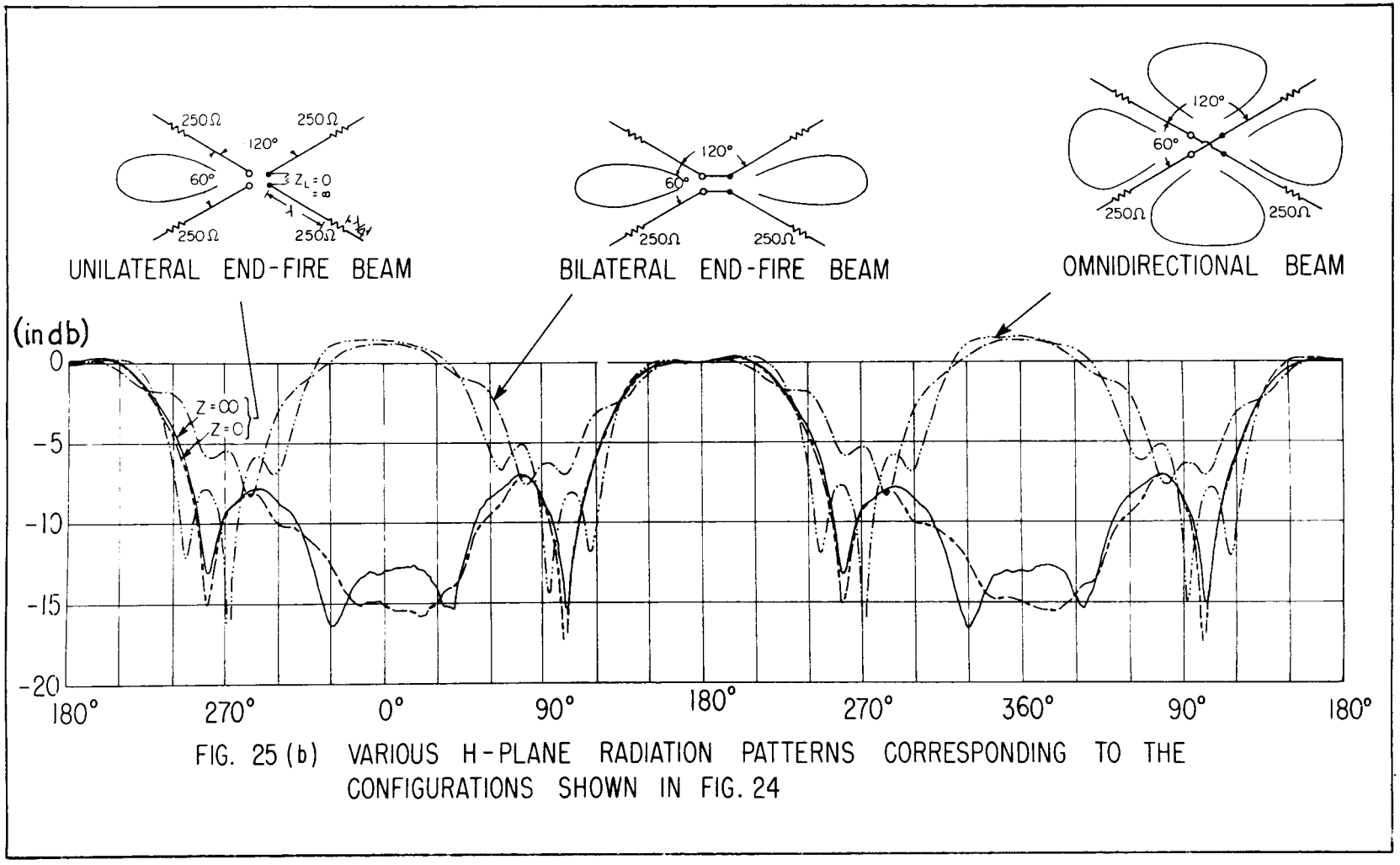

FIG. 25 (b) VARIOUS H-PLANE RADIATION PATTERNS CORRESPONDING TO THE CONFIGURATIONS SHOWN IN FIG. 24